TÉCNICO LISBOA

Investigations on the impact of membrane cleaning on the structure of a fouling layer from biorefining

Ana Sofia Caldas Vieira Gomes Correia

Thesis to obtain the Master of Science Degree in

Chemical Engineering

Supervisors: Prof. Frank Lipnizki (LU)

Prof. Maria Norberta de Pinho (IST)

Examination Committee

Chairperson: Prof. Cristina Fernandes (IST)

Supervisor: Prof. Frank Lipnizki (LU)

Members of the Committee: Prof. Moisés Pinto (IST)

Prof. Miguel Minhalma (ISEL)

November 2021

Preface

The work presented in this thesis was developed at the Department of Chemical Engineering of Lund University (Lund, Sweden), under the supervision of Prof. Frank Lipnizki and Dr. Gregor Rudolph, between February 2021 and August 2021 and within the Erasmus programme. The thesis was co-supervised by Prof. Maria Norberta de Pinho at Instituto Superior Técnico.

Acknowledgements

First of all, I would like to show my deepest gratitude to my supervisors Prof. Frank Lipnizki and Prof. Maria Norberta de Pinho for believing in my and making all this possible. Thank you so much Prof. Frank for the amazing opportunity of being part of the Membrane Group and work under your supervision and thank you for always being so kind and supportive. Prof. Norberta, your encouraging and guidance were essential for me to be able to pursue this work, thank you for looking after me and giving me the self-confidence that I needed.

Special thanks to Dr. Gregor Rudolph for helping me through every step of the way. Thank you Gregor for everything that you taught me, for pushing me outside of my comfort zone, and for being so patient and caring towards me. And most of all, thank you for always being there for me, I am beyond grateful for everything you have done for me and for my work.

Thank you to everyone from the Membrane Group, it was a pleasure to work with you all during my stay in Lund. To Mariona Battestini Vives, thank you for always helping me when I was in trouble and for cheering me up every day. To Dr. Basel Al-Rudainy for being so available to assist me with my technical issues. And of course, thank you to Omer Khalid for the friendship, and to Maja Lindblad for being the best office mate ever. My stay in Sweden would not have been the same without you both.

I would like to appreciate everyone at the Department of Chemical Engineering, Lund University, for making me feel so welcome, it was a thrill to share this life experience with you all.

I would like to thank my family for all the support during my journey in university. A special thank from the bottom of my heart to my parents for being my number one pillar of strength, you mean the world to me. Thank you also to my grandparents for always believing in me and for motivating me to pursue all my ambitions.

I wish to appreciate all my friends who stood by me during the ups and downs along the way, I could not have made it without you. Special thanks to my friends from Valsassina for your friendship over all these years. I am the luckiest person to have you by my side through every step of my life. I am extremely grateful for my friends from Técnico for being such an important part of my life in university, I am so proud of the journey we shared together.

Last but not least I would like to thank my boyfriend Pedro (M) for all the love and unconditional support, with you everything becomes easy and joyful.

Abstract

Nowadays, traditional pulp and paper mills must develop strategies to get the highest possible value from their process streams, to become more sustainable and improve revenues. To achieve that, they need to convert into lignocellulosic biorefineries.

Membrane technology has proven to be an effective method to separate and purify compounds from waste streams of pulp and paper mills. However, membrane fouling is still a challenging drawback that inhibits a wider implementation of membrane processes in this industry, as it decreases filtration capacity.

Membrane cleaning became crucial to remove foulants and to recover the membrane performance. Therefore, the aim of this work is to investigate the influence of the parameters temperature, duration and concentration of an alkaline cleaning agent on the cleaning success.

This study was conducted on polysulfone membranes fouled during ultrafiltration with thermomechanical pulping process water. The impact of the cleaning parameters was investigated with a Design of Experiment (DoE) approach. Additionally, the membrane surface and the fouling layer were analysed with contact angle measurements, Fourier transform infrared spectroscopy and Brunauer-Emmett-Teller analysis.

The evaluation of the DoE method revealed that concentration of the cleaning agent is the most relevant parameter. Moreover, the interaction between concentration and temperature displays a considerable influence in the cleaning efficiency.

Membrane analysis indicated that the main foulants attached to the membrane surface are polysaccharides in the form of hemicelluloses. They seem to be eliminated with some success by cleaning with an alkaline solution. Furthermore, an extensive development of pore blocking on the fouled membranes was detected.

Keywords: lignocellulosic biorefineries, thermomechanical pulping, ultrafiltration, membrane fouling, membrane cleaning, polysaccharides

Resumo

Atualmente, as fábricas tradicionais de papel e pasta celulósica têm de desenvolver estratégias para extrair o máximo de valor possível das suas correntes de processo, tornando-se mais sustentáveis e maximizando os seus lucros. Para tal, é necessário converterem-se em biorrefinarias lignocelulósicas.

As tecnologias de membranas provaram ser um método de filtração eficiente para separar e purificar componentes de correntes residuais provenientes de fábricas de papel e pasta celulósica. No entanto, o *fouling* das membranas é ainda uma desvantagem considerável que impede uma implementação mais abrangente dos processos de separação por membranas nesta indústria, visto que reduz a capacidade de filtração das mesmas.

A limpeza das membranas tornou-se então crucial para remover as partículas de *fouling* e para recuperar o desempenho das membranas. Posto isto, esta tese tem como objetivo investigar a influência dos parâmetros temperatura, duração e concentração de um agente de limpeza alcalino no sucesso da limpeza.

Este estudo foi realizado em membranas de polusulfona, que foram sujeitas a algum *fouling* devido à ultrafiltração de uma corrente de processo de uma fábrica de produção de pasta celulósica termomecânica. O impacto dos parâmetros de limpeza foi investigado com uma abordagem de *Design of Experiment* (DoE). Adicionalmente, a superfície das membranas e a camada de *fouling* foram analisadas através da medição dos ângulos de contacto, da espectroscopia de infravermelho com transformada de Fourier e da análise de Brunauer-Emmett-Teller.

A avaliação do método de DoE revelou que a concentração do agente de limpeza é o parâmetro mais relevante. Além disso, a interação entre a concentração e a temperatura também tem uma influência considerável na eficiência da limpeza.

As análises indicaram que as principais partículas de *fouling* ligadas à superfície das membranas são polissacarídeos sob a forma de hemiceluloses. Essas partículas aparentam ser eliminadas com algum sucesso quando limpas com uma solução alcalina. Foi também detetado um extenso desenvolvimento de bloqueio de poros nas membranas que sofreram algum *fouling*.

Palavras-chave: biorrefinarias lignocelulósicas, produção de pasta celulósica termomecânica, ultrafiltração, *fouling* das membranas, limpeza das membranas, polissacarídeos

List of Contents

List of Figures

List of Tables

Glossary

Abbreviations

BET: Brunauer-Emmett-Teller

BJH: Barrett, Joyner and Halenda

CCF: Central composite face-centered

CFV: Cross-flow velocity (m/s)

DoE: Design of Experiment

F&C: Filtration and centrifugation

FTIR: Fourier transform infrared spectroscopy

GGM: Galactoglucomannan

IFBR: Integrated forest biorefineries

MF: Microfiltration

NaOH: Sodium hydroxide

NF: Nanofiltration

NREL: National Renewable Energy Laboratory

NTU: Nephelometric turbidity unit

P: Permeability (L/(m^2.h.bar))

PES: Polyethersulfone

PSU: Polysulfone

PWF: Pure water flux (L/(m^2.h))

RO: Reverse osmosis

TMP: Transmembrane pressure (bar)

UF: Ultrafiltration

VR: Volume reduction (%)

Symbols

% (w/w): Weight percentage

$P_{conditioned}$ membrane: Pure water permeability of a conditioned membrane (L/(m^2.h.bar))

P_{fouled} membrane: Pure water permeability of a fouled membrane (L/(m^2.h.bar))

$P_{cleaned}$ membrane: Pure water permeability of a cleaned membrane (L/(m^2.h.bar))

$m_{permeate}$: Permeate mass (g)

$A_{membrane}$: Membrane area (m^2)

t: Time (h)

ρ: Density (g/L)

p_{feed}: Feed pressure (bar)

$p_{permeate}$: Permeate pressure (bar)

$p_{retentate}$: Retentate pressure (bar)

J: Flux (L/(m^2.h))

ε: Absorptivity (L/(g.cm))

1. Literature Review

This chapter gives an insight about membrane technologies and their applications regarding pulp and paper industry. A comprehensive review on membrane fouling and membrane cleaning is given along with a brief understanding about Design of Experiment (DoE). This chapter also highlights analytical techniques to further characterize the membrane surface. Finally, the aim of this these is presented.

1.1. Pulp and Paper Mills

The manufacturing of paper consists of a two-step operation: first fibrous raw material is separated into a pulp and then the pulp is transformed to produce paper. Pulp can be produced by chemical or mechanical processes **[1]**. This work focusses on thermomechanical pulping, where pulp is shortly preheated and then it is conducted to steam pressurized refiners **[2]**.

1.2. Lignocellulosic Biorefineries

About 95% of wood biomass is used to produce paper in thermomechanical pulp mills, while the remaining 5% are discharged and wasted **[3]**. Consequently, pulp and paper mills have started to consider other options to increase profitability and competitiveness, hence the intention of converting existing pulp and paper mills into integrated forest biorefineries (IFBR) emerged.

Besides pulp and paper, an IFBR generates a wide spectrum of bio-based products and biofuels by processing lignocellulosic biomass, i.e., wood (**Figure 1**). The transformation into an IFBR would improve the diversity of the products and therefore would create new revenues **[4]**.

1.2.1. Lignocellulosic Biomass

Extractives, cellulose, hemicelluloses and lignin are the main components of lignocellulosic biomass. Extractives are lipophilic substances that are soluble in organic solvents. Cellulose and hemicelluloses are both polysaccharides that provide support in the plant cell wall. Lignin is a structural polymer in the tissues of most plants. Galactoglucomannan (GGM) represents the major hemicellulose in softwood, and it has a great potential as a raw material for bio-based products **[5]**.

In a thermomechanical pulp and paper mill, cellulose is used in the production of pulp and paper, while hemicelluloses are underutilized, instead of being converted into value-added products, including hydrogels, oxygen barrier films in food packaging and emulsion stabilizers. Lignin has a great potential regarding biofuels production due to its heat value **[4]**.

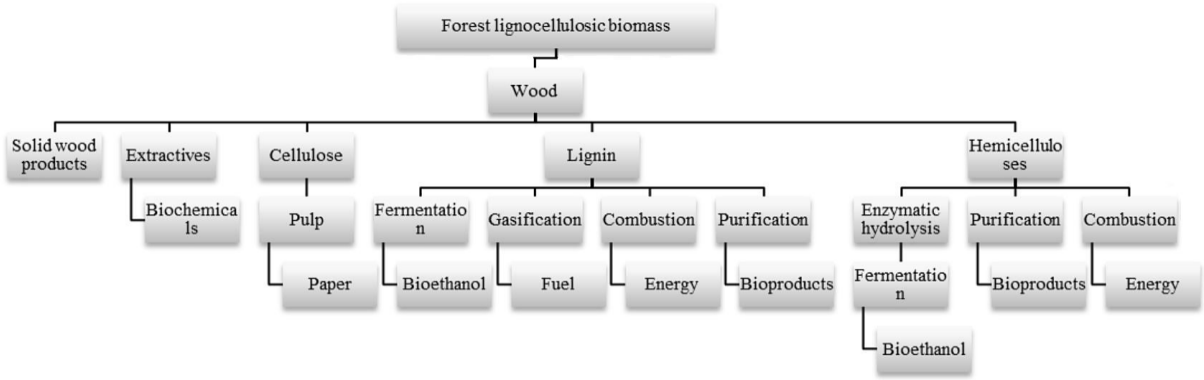

Figure 1 - Schematic of the range of potential products from IFBR. Adapted from **[4]**.

1.3. Membrane Separation Processes

Membrane filtration is a promising method to put the concept of an IFBR into action, since it provides an efficient separation and fractionation **[4]**. Membrane technologies demand low energy when compared to conventional separation technologies, such as centrifugation, drying and evaporation **[6]**. Membrane separation processes are also easily scaled-up and implemented in the existing operating units **[4]**, as they have a relatively low footprint **[7]**.

1.3.1. Pressure Driven Membrane Processes

In pressure driven membrane processes, transmembrane pressure (TMP) is the driving force. These processes can be classified into four types, according to working pressure and membrane pore size **[8]** (**Figure 2**): microfiltration (MF), ultrafiltration (UF), nanofiltration (NF) and reverse osmosis (RO). Each process has different pressure requirements due to the difference in membrane pore size **[9]**.

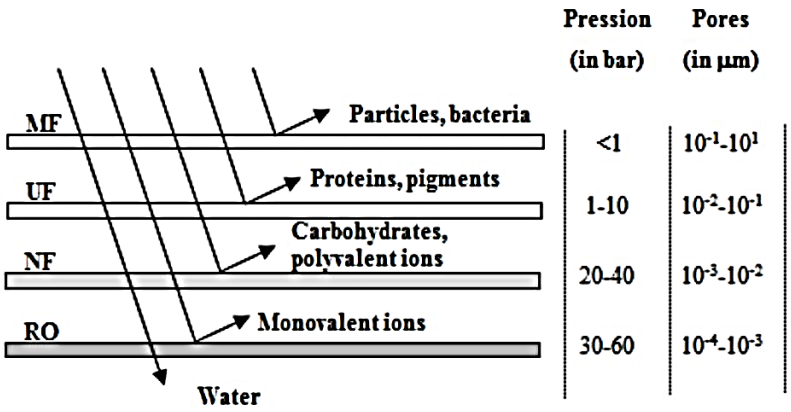

Figure 2 - Pressure driven membrane processes **[10]**.

In biorefinery process streams (**Figure 3**), solids like fibres are separated by filtration or centrifugation (F&C). Colloidal matter such as extractives and suspended solids are removed by MF. Macro molecules like hemicelluloses and proteins are recovered by UF. Lignin and monosaccharides are isolated by NF. Salts are concentrated by RO **[11]**.

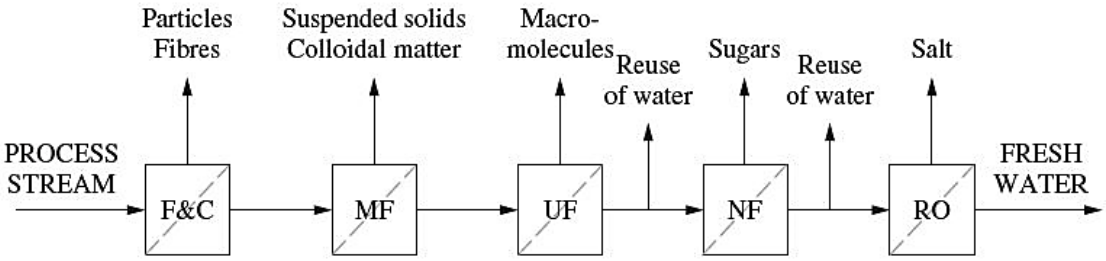

Figure 3 - Schematic of the filtration processes of components from biorefinery process streams **[11]**.

1.3.2. Ultrafiltration

This work is based on an UF process. UF technology has a wide range of applications due to its outstanding selectivity and it allows to efficiently recover and purify valuable compounds from pulp and paper mills waste streams, such as hemicelluloses and lignin **[4]**.

1.3.3. Operating Parameters

The operating parameters must be optimized according to each specific situation to increase membrane performance and reduce process costs. For UF, TMP, cross-flow velocity (CFV), operating temperature, and pH of the solutions are the main operating parameters. Generally, an increase in TMP, CFV and temperature causes an increase in flux, which is desirable. However, the energy required increases as well. For that reason, achieving a balance between low energy demand and high flux is essential **[11]**.

1.4. Membrane Fouling

Membrane fouling is defined as an agglomeration of undesirable matter (foulants) on the membrane surface and into the membrane pores. A strong indication of fouling is a decrease in flux over time, during constant pressure operation **[12]**. It is essentially influenced by hydrophobic/hydrophilic and electrostatic interactions between foulants and membranes **[13]**.

Membrane fouling is what prevents the adoption of membrane technology in a large scale in biorefineries **[4]**. Fouling leads to a decrease in membrane lifetime and reduction in filtration capacity. Furthermore, it leads to higher operation costs due to membrane replacements, which represents 25 to 40% of the total membrane equipment cost, and membrane cleaning, which accounts for 15 to 20% of the operating expenses **[14]**.

Membrane fouling can be classified as removable, irremovable and irreversible. In case of removable fouling, loosely foulants are attached on the membrane surface, which can be removed by physical cleaning by e.g., backflushing. Irremovable fouling can only be removed by chemical cleaning. Irreversible fouling is not possible to be removed by any kind of cleaning **[15]**.

There is a lack of information regarding the nature of foulants from pulp and paper wastewaters because of the complexity of process streams in the forest industry. Although, there are few studies

about membrane fouling in IFBR **[4]**. Furthermore, identifying the foulants deposited on the membrane surface can be challenging, since they usually represent small amounts **[15]**. However, it has been reported that wood extractives from pulp and paper mill waste streams like fatty acids and resin cause membrane fouling **[16]**. It has also been shown that polysaccharides are one of the main foulants in pulp mill process streams **[15]**.

1.4.1. Fouling Mechanisms

Fouling mechanisms can be classified into three types: adsorption, pore blocking and cake layer formation (**Figure 4**). Pore blocking occurs when the size of the solute molecules is similar to the size of the membrane pores **[6]**. Cake layer formation takes place if the solute molecules are larger than the membrane pores. Adsorption occurs if the solute molecules are smaller than the membrane pores instead. During this phenomenon, the solute molecules adsorb onto the pore wall, reducing the pore diameter **[11]**.

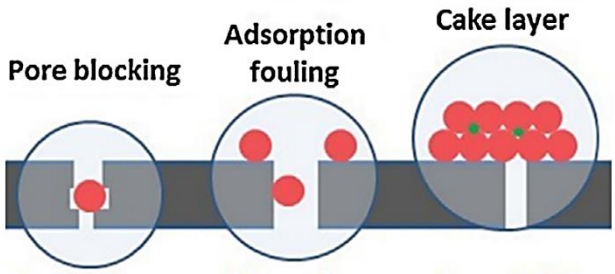

Figure 4 - Illustration of the three types of membrane fouling. Adapted from **[17]**.

Typically, the membrane-foulant and the foulant-foulant interactions have a significant impact on the fouling layer formation. The adsorption of foulants on the pore walls and on the membrane surface depends on the membrane-foulant interactions. Foulant-foulant interaction interferes with the development of the fouling layer caused by the continuous sedimentation and accumulation of foulants **[12]**.

1.4.2. Influence of Filtration Conditions

The operating conditions during the filtration have a substantial impact on fouling issues **[3]**.

1.4.2.1. Cross-flow Filtration

Cross flow filtration is usually promoted over dead-end filtration, as the feed solution flows tangentially to the membrane surface. This increases the shear force above the membrane and thus, reduces the risk of fouling, since only a small portion of particles accumulates on top of the membrane. On the other hand, dead-end filtration is more susceptible to membrane fouling, as the feed solution

flows perpendicularly to the membrane surface (**Figure 5**). For that reason, dead-end mode is frequently used to treat feed solutions with a minimal risk of membrane fouling, while cross-flow mode is more suitable when filtrating feed solutions with a high content of suspended solids, colloidal matter and organic components **[8]**.

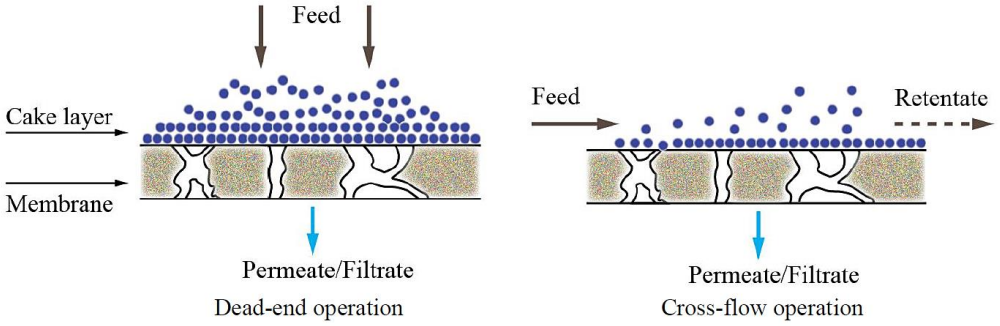

Figure 5 - Illustration of the membrane filtration operation modes **[8]**.

1.4.2.2. Membrane Material

Polysulfone (PSU) and polyethersulfone (PES) are commonly used polymeric materials for UF membranes used in biorefinery **[12]**. Utilizing polymeric membranes offers several advantages, since they have a considerable heat, chemical, and mechanical resistance **[14]**. However, PSU and PES have a hydrophobic character, increasing the vulnerability of the membranes regarding fouling caused by wood extractives **[12]**. Consequently, PSU and PES membranes need to be adjusted/coated so they are more hydrophilic **[18]**.

1.4.2.3. Membrane Module Geometries

The different membrane module geometries have a significant impact on fouling and channel blockage. It can be classified into four types: tubular, flat-sheet, spiral-wound and hollow fibre (**Table 1**). Spiral-wound and hollow fibre modules accuse the highest fouling propensity and the lowest cleanability. However, they are widely employed, since they have a high ratio of membrane area to footprint and therefore require lower investment and energetic expenses **[14]**.

Table 1 - Comparison between the different module geometries. Adapted from **[14]**.

Module Geometry	**Tubular**	**Flat-sheet**	**Spiral-wound**	**Hollow fibre**
Investment Costs (€/m^2, 2000)	43-172	43-172	4-86	4-17
Energetic Costs	High	Moderate	Low	Low
Fouling	Low	Low	Moderate	High
Cleaning	Excellent	Good	Moderate	Moderate

1.5. Membrane Cleaning

Due to the negative effects of membrane fouling on the filtration process over time, regularly membrane cleaning becomes a necessary procedure **[15]**. Membrane cleaning is described as the removal of substances and material that are not an intrinsic part of the membrane **[14]**. It is imperative to implement regular cleanings into membrane plants to avoid irreversible fouling **[19]**.

Physical cleaning removes visible dirtiness, whereas chemical cleaning eliminates all impurities and biological cleaning destroys living microorganisms **[20]**.

A cleaning cycle usually includes several steps, such as **[11]**:

- Eliminate the product from the system
- Rinse the system with water
- Clean the system (one or multiple steps)
- Rinse again the system with water
- Disinfect the system (if needed)

Typically, a low water flux is an indicator that the cleaning was not sufficient. However, a good water flux does not mean that the membrane completely recovered its filtration efficiency. Temperature and duration along with concentration and type of cleaning agent represent the most important cleaning variables **[20]**.

Cleaning conditions are often selected based on trial-and-error procedures **[19]**, although cleaning parameters and its optimization have been investigated more profoundly since the 1990s, aiming to reduce operating costs while increasing membrane efficiency **[14]**.

1.5.1. Chemical Cleaning

Chemical cleaning is a heterogeneous reaction between the fouling layer and the cleaning agent and it generally consists of the following steps **[13]**:

- Cleaning agent is added to the feed tank
- Cleaning agent interacts with the fouled surface
- Cleaning agent is transported through the fouled layer
- Cleaning agent looses and dissolves foulants
- Products originated by the cleaning reaction are conducted back to the interface
- Products originated by the cleaning reaction are transported back to the feed

Cleaning agents used for membrane cleaning are mainly acids, alkalis, detergents **[4],** or enzymes. Often, a sequence with different cleaning agents is required to achieve a satisfactory cleaning. Drawbacks of chemical cleaning are originating pollution **[11]** and destroying membrane materials if the cleaning conditions are too harsh **[14]**.

An adequate cleaning agent should demonstrate a good performance regarding dissolving and retaining fouling particles in dispersion, without damaging the membrane and the system. It is also convenient to use a cleaning agent that is easily rinsed from the system and that remains chemically stable during the cleaning reaction. Lastly, safety and cost are important factors to consider when it comes to selecting a proper cleaning agent **[20]**.

1.6. Membrane Analysis

In this work, contact angle measurements, Fourier Transform Infrared Spectroscopy (FTIR) and Brunauer-Emmett-Teller (BET) analysis have been applied to further characterise membrane fouling caused by thermomechanical pulping process water **[12]**.

1.6.1. Contact Angle Measurements

Contact angle measurements are a valuable method to characterise a membrane regarding its hydrophilicity or hydrophobicity properties. A high water affinity results in a low contact angle, therefore fouling can be identified due to variation in the contact caused by alterations in membrane properties.

In membrane science, the most common approach to determine a contact angle is by using the sessile drop technique (**Figure 6**), which considers the contact angle between a water droplet and a solid surface in air **[21]**. The shape of the water drop on the solid surface depends on the surface tension and the nature of the surface **[22]**.

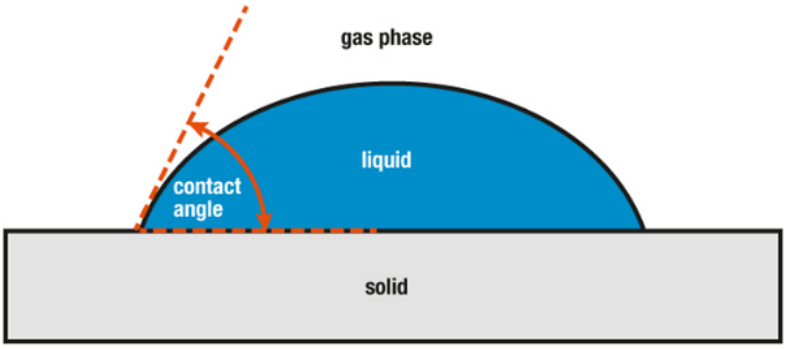

Figure 6 - Illustration of a contact angle measurement in accordance with the sessile drop technique **[22].**

1.6.2. Fourier Transform Infrared Spectroscopy

FTIR is one of the most important spectroscopy technologies utilized to identify organic compounds on pristine, fouled and cleaned membranes. Spectra obtain by FTIR show the differences in absorbance corresponding to each wavelength and each peak is assigned to a functional group **[14]**.

FTIR analysis is a convenient method to contribute with further knowledge about the chemical nature of foulants **[12]**.

1.6.3. Brunauer-Emmett-Teller Analysis

BET analysis can contribute with structural information regarding the fouling layer, as it provides crucial information about surface area and porosity of microporous (< 2 nm), mesoporous (2 - 50 nm) and even macroporous (> 50 nm) surfaces. BET technique is extremely useful since the conventional flux measurements cannot provide reliable information whether changes in filtration performance are a consequence of adsorption, pore blocking or cake layer formation **[12]**.

BET theory (**Figure 7**) is based on the adsorption and desorption of a gas on a solid surface and there are multiple factors that interfere with the process, such as pressure, temperature, and properties of the material. First, the sample tube is evacuated. Thereafter, the pressure is slowly increased by gassing in nitrogen into the sample tube. At low gas pressures, the gas molecules will adsorb onto the material surface at isolated spots and develop towards a monolayer. With increasing gas pressure, multilayer adsorption occurs. When the gas pressure is high enough, the gas molecules start to condensate, and the pores are filled up with a liquid phase. This happens during the adsorption step. Afterwards, the gas pressure is reduced again and the desorption can be studied. The difference between the adsorption and desorption kinetics gives indications about the surface area and porosity of the investigated sample **[23]**.

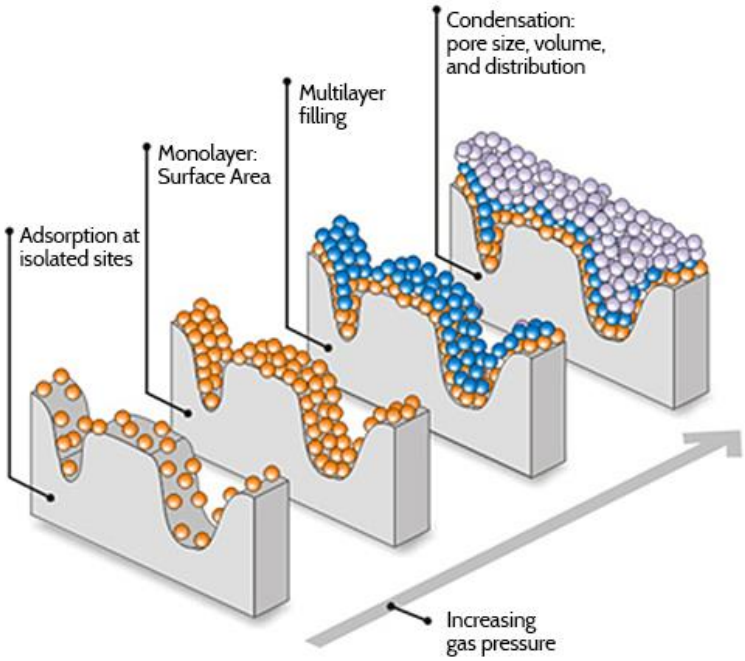

Figure 7 - Schematic of BET adsorption theory **[24]**.

1.7. Design of Experiment

DoE provides an organized approach to study the interaction of multiple factors on which an experiment depends on, representing a vital tool to optimize processes in scientific field **[25]**.

When a study involves several parameters, it is frequent to obtain a great amount of data hard to analyse and it usually demands a lot of worthless trials. With DoE it is possible to collect only relevant data performing the minimum experimental runs, reducing time and costs **[14]** by establishing a

correlation between factors (independent variables) and responses (dependent variables) with mathematical models **[26]**.

It is necessary to select a suitable model before implementing this methodology. First order designs (factorial designs) cannot be used to analyse data, such as temperature and pH, that produces non-linear effects on the response. Quadratic designs are qualified to represent more complex systems which cannot be defined by a linear equation. Then, statistical evaluation confirms if the regression surface obtained by the model provides an accurate representation of the authentic system **[14]**.

DoE has been used to study and optimize membrane cleaning efficiency of UF membranes. It is an efficient method to investigate several parameters at the same time and identify the main factors and their interactions. With statistical analysis, the less significant parameters can be identified and discarded from the study, allowing to focus only on the most relevant ones when developing the model **[19,13]**.

1.8. Scope of the Thesis and Objectives

There is a great demand for improving the knowledge about optimizing membrane cleaning. In general, many cleaning protocols used in industry are not sustained by a theoretical explanation and are only based on trial-and-error studies **[14]**.

The main purpose of this thesis is to contribute to the progress of the state of the art of membrane cleaning with a better understanding about the impact of the parameters temperature, duration and concentration of a commonly used cleaning agent on the cleaning performance. This will be done on the example of membrane fouling during UF of process water from thermomechanical pulping. The work aims to provide an optimized cleaning procedure plus a comprehensive understanding on the structure and composition of a fouling layer caused by thermomechanical pulping process water.

2. Materials and Methods

In this chapter, the materials and experimental procedures adopted in this study are described. The calculations and analytical methods used to process the experimental data are also reported.

2.1. Membrane and Filtration Equipment

The membranes used in this study were commercial PSU UF membranes of the type UFX5-pHt (Alfa Laval, Denmark) with a nominal molecular weight cut-off of 5000 g/mole. The membranes are permanently hydrophilized. The membranes used in the first 11 experiments (**Table 2**) were flat-sheet membranes from one batch. The ones used in the last 8 experiments (**Table 3**) were originated from a spiral-wound module which was opened and cut into several flat-sheets.

All the experiments were performed in a cross-flow module with three membrane samples in parallel (**Figure 8**). The effective membrane area of each sample was 1960 mm^2.

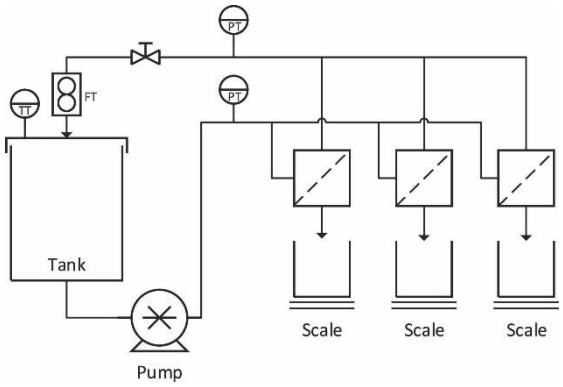

Figure 8 - Schematic of a cross-flow mode membrane filtration set-up **[27]**. FT = flow meter, PT = pressure transmitter, TT = temperature transmitter.

2.2. Feed Solution

Diluted retentate after MF of process water from thermomechanical pulping (Stora Enso, Sweden) was used as a feed solution to foul the membranes. Suspended solids were removed with a drum filter directly at the pulp mill.

The initial volume reduction (VR), defined as the ratio between the permeate volume and the feed volume, of the MF retentate was 98%. The retentate was diluted to reach its original concentration of solute and the pH of the solution was adjusted with the help of a HI 8424 pH meter (Hanna, US), by adding 50-200 µL of 99,8% acetic acid glacial (VWR Chemicals, Germany) for 5 L of solution, to remain unchanged (around 4).

2.3. Ultrafiltration Solutions Analysis

The feed solution together with the permeate and the retentate obtain from UF with the membranes from the flat-sheet batch were analysed according to the standardized National Renewable Energy Laboratory (NREL) analytical procedures **[28, 29]**. All analyses were performed in triplicates,

except for the Klason lignin that was only analysed for one sample per solution. Procedures described below were based on analysis procedures stated in **[30]**.

The feed solution and the retentate were both 3-fold diluted and turbidity was then determined with a 2100P ISO turbidimeter (HACH, USA). Total solids and ash were determined after weighting and drying the samples in an oven for 24 hours at 105 ˚C. After cooling down to ambient temperature, the samples were weighted again. The difference in weight is the amount of total solids. The dry sample was then heated to 575 ˚C for 3 hours, cooled down to ambient temperature, and finally weighted again. The difference in weight is the amount of ash.

The feed solution and the retentate were 7-fold and 10-fold diluted, respectively, and total lignin was afterwards determined by using an UV-1800 spectrophotometer (Shimadzu, Japan) at a wavelength of 280 nm. Total lignin was then calculated, assuming an absorptivity (ε) of 17.8 L/(g.cm). To determine acidic lignin and Klason lignin, the samples were acid hydrolysed with 1.5 mL of 72% sulfuric acid (Chem-Lab, Belgium) in an autoclave DX-150 (Systec, Germany). Subsequently, the precipitate was separated by vacuum filtration in filter cups that were previously dried in an oven for 24 hours at 105 ˚C and then weighted. The difference in weight is the Klason (insoluble) lignin. The liquid fraction from the vacuum filtration was partially utilized to determine the acidic (soluble) lignin, by using an UV-1800 spectrophotometer (Shimadzu, Japan) at a wavelength of 320 nm and none of the solutions were diluted. Acidic lignin was subsequently calculated, assuming an absorptivity (ε) of 30 L/(g.cm).

The feed solution and the retentate were 20-fold and 10-fold diluted, respectively, and monosaccharides were analysed from the liquid fraction from the vacuum filtration with a ICS-3000 high-performance anion-exchange chromatography system with pulsed amperometric detection (Dionex, USA) coupled to a Carbo Pac PA1 analytical column. The monosaccharides D-glucose, D-galactose, D-mannose, D-xylose and L-arabinose (Fluka Chemie AG, Switzerland) were used as standards.

2.4. Experimental Procedures

Procedures described in the subchapters Membrane Conditioning and Membrane Fouling are based on membrane filtration procedures that can be found in **[27]**.

2.4.1. Membrane Conditioning

Before each fouling and cleaning experiment, the membranes were conditioned to remove storage chemicals, such as glycerine. The commonly used alkaline cleaning agent, Ultrasil 10 (Ecolab, Germany), was used for this.

Conditioning was performed with 5 L of a 1% (w/w) solution of Ultrasil 10, at 50 ˚C. Firstly, the system was heated with 4 L of deionized water to 50 ˚C, with a TMP of 2 bar and a CFV of 0.28 m/s. Then, 1 L of Ultrasil 10 solution was added, TMP and CFV were adjusted to their initial values and conditioning was conducted for 1 hour, recirculating both the permeate and the retentate.

After conditioning, the system was rinsed with 20 L of deionized water at 50 ˚C, while both the permeate and the retentate went to the drain. Rinsing was carried out without any TMP and a CFV of 0.28 m/s. Then, the system was filled with another 5 L of deionized water at 50 ˚C. A TMP of 2 bar and a CFV of 0.28 m/s were applied for 10 min, while the permeate went to the drain and the retentate was

recirculated. After that, rinsing was repeated with an extra 20 L of deionized water at ambient temperature, without applying a TMP and a CFV of 0.28 m/s, while both the permeate and the retentate went to the drain. Finally, the system was rinsed with another 10 L of deionized water under the same conditions as the ones on the previously rinsing step.

In this research, the TMP was calculated by the following equation **[11]**:

$$TPM = \frac{p_{feed} + p_{retentate}}{2} - p_{permeate} \quad \textbf{(1)}$$

2.4.2. Membrane Fouling

The conditioned membranes were fouled by UF of the feed solution. First, the system was heated with 4 L of deionized water to 50 ℃ without applying a TMP, and a CFV of 0.28 m/s, recirculating both the permeate and the retentate. At the same time, 5 L of fouling solution were heated in a glass beaker to 50 ℃ on a RET basic magnetic stirrer (Ika, Germany), with the help of an electric heater. When both the system and the fouling solution reached 50 ℃, the feed tank was emptied and the fouling solution was added. Then, the system was started at a low CFV and around 1 L of retentate was collected in a beaker, to make sure that the water remaining inside the system (dead volume) was removed before the filtration started. Thereafter the retentate was recirculated. At a low CFV, the system was heated to 70 ℃, recirculating both, the permeate and the retentate. When the system reached the temperature of 70 ℃, the CFV was adjusted to 0.28 m/s and the TMP was slowly increased to 2 bar. At this point, the feed tank was covered with a lid, to avoid evaporation of the liquid inside the tank. UF with recirculation was conducted for 26 hours.

For the membranes from the flat-sheet batch, after 26 hours the recirculation was stopped and a concentration was initiated, where the permeate was collected inside beakers for 1 hour. This was done to intensify the fouling further. For the membranes originated from the spiral-wound module, after the 26 hours of recirculation, no concentration was conducted as fouling was already severe enough.

Lastly, the system was shut down and the feed tank was emptied. In order to remove all the fouling solution inside the system, the same rinsing protocol used as after membrane conditioning was followed.

2.4.3. Membrane Cleaning

Three cleaning parameters were studied in this project: temperature, concentration, and duration. The values of those parameters for each cleaning experiment are displayed on **Tables 2 and 3**. They were arranged based on the requirements showed on **Table 4**. For all cleaning experiments, the TMP was kept constant at 2 bar and the CFV at 0.28 m/s. Subsequently to the cleaning, the same rinsing protocol used as for membrane conditioning was followed.

Table 2 - Experimental parameters of the cleaning experiments performed on the membranes from the flat-sheet batch.

Experiment	Cleaning Temperature (˚C)	Cleaning Concentration (%) *	Cleaning Duration (min)
1	50	0.25	60
2	70	0.5	60
3	50	0.5	35
4	30	0.5	10
5	70	0	60
6	30	0.5	60
7	30	0	10
8	50	0.25	35
9	50	0	35
10	50	0.25	35
11	30	0.25	35

*% (w/w) Ultrasil 10

Table 3 - Experimental parameters of the cleaning experiments performed on the membranes originated from the spiral-wound module.

Experiment	Cleaning Temperature (˚C)	Cleaning Concentration (%) *	Cleaning Duration (min)
12	70	0.5	10
13	30	0	60
14	70	0	10
15	70	0.25	35
16	70	0.5	60
17	50	0.25	35
18	30	0	10
19	30	0.5	60

*% (w/w) Ultrasil 10

2.4.4. Pure Water Flux Measurements

Fouling and cleaning efficiency were assessed based on pure water flux (PWF) measurements. The PWF was determined after membrane conditioning, membrane fouling, and membrane cleaning, respectively, for the three membranes assembled on the UF equipment. For this, the permeate was collected inside beakers and continuously weighed with an electronic balance. The PWF was measured at 30 ˚C, 0.28 m/s, and at four TMPs: 0.5, 1, 1.5, and 2 bar. The flux (J) was calculated based on the following equation:

$$J = \frac{m_{permeate}}{A_{membrane} \times t \times \rho} \quad \textbf{(2)}$$

The mass of permeate ($m_{permeate}$) was recorded during each measurement, and its density (ρ) was assumed to be 1000 g/L. The time (t) of each measurement was 5 minutes and the effective membrane area of each sample ($A_{membrane}$) was 1960 mm^2.

2.4.4.1. Fouling Factor and Cleaning Success

The average flux of the three membranes assembled on the UF equipment was calculated for each pressure point. A linear regression of the correlation between the average flux and the TMP (0.5, 1, 1.5, and 2 bar) was determined. The obtained slope corresponds to the permeability (P).

The fouling factor was calculated by the following equation:

$$Fouling\ Factor = \frac{P_{conditioned\ membrane} - P_{fouled\ membrane}}{P_{conditioned\ membrane}} \quad \textbf{(3)}$$

The cleaning success was calculated by the following equation:

$$Cleaning\ Success = \frac{P_{cleaned\ membrane}}{P_{conditioned\ membrane}} \quad \textbf{(4)}$$

2.5. Design of Experiment

The central composite face-centred (CCF) design was selected for the DoE evaluation. In CCF, there is a cuboidal design space with points centred on each face of the cube, on each vertex and on the centre (**Figure 9A**). This design requires three levels of each factor: high level, low level and average (**Table 4**). Three cleaning parameters (factors) were investigated: temperature, concentration of the cleaning agent (Ultrasil 10), and duration. These three factors are represented by three axes (**Figure 9B**) and each level varies between -1 and 1.

The CCF method was executed with the software MODDE 13 Pro (Startorius, version 13.0.1.27179, Germany). This model has the purpose of studying and optimizing the relationship between multiple input factors (the three investigated cleaning parameters) and one output response (cleaning success). The input factors and their range of values were set up according to **Tables 2 and 3**. For the output response, a range between 0.3 and 1.3 and a target of 1 was chosen.

Two DoE studies were carried out, one for the membranes from the flat-sheet batch and another one for the membranes originated from the spiral-wound module. Ideally, each study should include 16 data points: the 15 data points illustrated by **Figure 9A** and a replicated centre point, to estimate the experimental error. However, it was only possible to perform 11 experiments for the first batch of membranes and 8 experiments for the second batch.

Table 4 - Leverage of the three cleaning parameters for the DoE setup.

Design Variable	Low Level	Average	High Level
Temperature (°C)	30	50	70
Concentration (%*)	0	0.25	0.5
Duration (min)	10	35	60

*% (w/w) Ultrasil 10

Figure 9 - CCF space design with the data points (**A**) and the three cleaning factors, represented by three axes (**B**).

2.6. Membrane Analysis

All membrane samples were stored and dried in an oven at 30 °C until they were further analysed. Investigated were the hydrophobicity of the membrane surfaces by the water contact angle measurements, the chemical composition of the membrane surfaces by attenuated FTIR, and the inner area and volume of the membrane samples by BET analysis.

2.6.1. Contact Angle Measurements

Contact angle measurements were performed according to the sessile drop technique on the three membrane samples of each experiment, with a drop and bubble shape tensiometer PAT-1M (SINTERFACE Technologies, Germany) and the software PAT-1M (SINTERFACE Technologies, version 1.6.0.744, Germany). A water droplet with a volume of 5-6 mm^3 was dropped onto a membrane sample with an approximated area of 100 mm^2. The measurements were conducted at room temperature for 60 seconds. The right and the left angle of each sample were determined by the average of the last 20 data points of each measurement. Then, the contact angle per sample was calculated by the average of the right and the left angle. Finally, the contact angle per experiment was obtained by the average of the contact angles of the three membrane samples.

2.6.2. Fourier Transform Infrared Spectroscopy

FTIR analysis were performed on the three membrane samples (approximated area of 100 mm^2) of each experiment to characterize the chemical composition of the sample surfaces. The

measurements were executed with a spectrometer ALPHA II (Bruker, Denmark) and with the software OPUS (Bruker, version 8.5.29, Denmark). The absorbance for each sample was measured within the wavenumber range from 400 to 4000 cm^{-1} and 72 scans were recorded with a resolution of 2 cm^{-1}. It was measured a background signal that was subtracted from the sample spectra. The spectra were base line corrected, and the absorbance data was then converted to transmittance for better comparison.

2.6.3. Brunauer-Emmett-Teller Analysis

BET analysis were conducted with a 3Flex surface characterization analyser (Micromeritics, USA). Before the analysis, the membranes were cut into small pieces and degassed at 50 ◦C for 12 hours in a smart VacPrep 067 degassing unit (Micromeritics, USA). Adsorption and desorption isotherms of nitrogen gas were recorded at -196 ◦C (boiling point of nitrogen). The data was evaluated with the software 3Flex (Micromeritics, version 5.02, USA).

The presented data was originated from the desorption branch of the obtained isotherms. Pore area and pore volume distributions were determined by the Barrett, Joyner and Halenda (BJH) method.

3. Results and Discussion

This chapter describes and discusses the results obtained from the ultrafiltration solutions analysis, membrane cleaning, DoE evaluation and membrane analysis.

3.1. Ultrafiltration Solutions Analysis

Analysis performed on the feed solution and on the permeate and retentate obtained from UF with the membranes from the flat-sheet batch are presented in **Table 5**. The turbidity measurements seem unreasonable since the turbidity of the feed solution is higher than the turbidity of the retentate. The measurement was repeated several times resulting in similar values. So far, the results cannot be explained. It has been shown that the turbidity of TMP process water after extracting suspended solids is related to the concentration of resins **[15]**, however the concentration of resigns should be higher in the retentate, where they are retained by UF.

The amount of ash found in the solutions is insignificant, since any ash was found in the feed solution, which suggests that the trace amounts of ash found in the permeate and retentate are due to experimental errors. The majority of lignin after UF was detected in the retentate, supporting the theory that this compound can be successfully retained by UF **[31]**.

Table 5 - Composition of the feed solution (diluted retentate after MF of process water from thermomechanical pulping) and of the permeate and retentate after UF of the feed solution with the membranes from the flat-sheet batch.

Solution	Turbidity (NTU) *	Dry Solids (mg/g)	Ash (mg/g)	Total Lignin (g/L)	Acidic Lignin (g/L)	Klason Lignin (mg/g)
Feed	409.3	2.52	0.00	0.34	0.02	0.33
Permeate	1.0	0.10	0.04	0.02	0.01	0.07
Retentate	319.7	5.12	0.05	0.37	0.02	0.39

* Nephelometric turbidity unit

Table 6 displays the concentration of monosaccharides measured in the feed solution and in the permeate and retentate obtained by UF with the membranes from the flat-sheet batch. Mannose, glucose and galactose were the monosaccharides detected in the feed solution and in the retentate. This was expected, as GGM is the main hemicellulose in softwood **[5],** and it is composed of those three monomers. Only trace amounts of arabinose were found and xylose was not detected. Most of the GGM was retained by UF, since only negligible amounts of mannose and glucose were in measured in UF permeate.

Table 6 - Concentration of monosaccharides of the feed solution (diluted retentate after MF of process water from thermomechanical pulping) and of the permeate and retentate after UF of the feed solution with the membranes from the flat-sheet batch.

Solution	Mannose (g/L)	Galactose (g/L)	Glucose (g/L)	Xylose (g/L)	Arabinose (g/L)	Total Sugars (g/L)
Feed	0.29	0.14	0.16	0.00	0.02	0.62
Permeate	0.01	0.00	0.01	0.00	0.00	0.02
Retentate	0.69	0.32	0.35	0.00	0.08	1.44

3.2. Membrane Cleaning

Tables 7 and 8 show an overview of the results from the fouling and cleaning experiments. The fouling factor and the cleaning success for each experiment were calculated according to **Equations 3 and 4**. The fouling factor was an important indicator of the fouling efficiency. As shown in the **Tables 7 and 8**, the fouling factor was lower for the membranes from the flat-sheet batch. It appeared as if the fouling was less severe and easier to remove, therefore the cleaning success was higher for the membranes of this batch.

Table 7 - Experimental parameters, fouling factor and cleaning success calculated with **Equations 3 and 4** of the cleaning experiments performed on the membranes from the flat-sheet batch.

Experiment	Cleaning Temperature (˚C)	Cleaning Concentration (%) *	Cleaning Duration (min)	Fouling Factor (-)	Cleaning Success (-)
1	50	0.25	60	0.266	1.144
2	70	0.5	60	0.090	1.721
3	50	0.5	35	0.135	1.191
4	30	0.5	10	0.114	1.331
5	70	0	60	0.225	0.961
6	30	0.5	60	0.158	1.229
7	30	0	10	0.115	0.952
8	50	0.25	35	0.108	1.280
9	50	0	35	0.124	0.972
10	50	0.25	35	0.215	1.237
11	30	0.25	35	0.160	1.311

*% (w/w) Ultrasil 10

Table 8 - Experimental parameters, fouling factor and cleaning success calculated with **Equations 3 and 4** of the cleaning experiments performed on the membranes originated from the spiral-wound module.

Experiment	Cleaning Temperature (˚C)	Cleaning Concentration (%) *	Cleaning Duration (min)	Fouling Factor (-)	Cleaning Success (-)
12	70	0.5	10	0.928	0.625
13	30	0	60	0.912	0.106
14	70	0	10	0.933	0.102
15	70	0.25	35	0.920	0.364
16	70	0.5	60	0.933	0.493
17	50	0.25	35	0.903	0.190
18	30	0	10	0.916	0.064
19	30	0.5	60	0.933	0.145

*% (w/w) Ultrasil 10

3.2.1. Design of Experiment

The CCF model was implemented with the software MODDE 13 Pro (Satorius, Germany) based on the cleaning parameters (inputs) and the cleaning success (output) from **Tables 7 and 8**.

Figures 10 and 11 present the observed versus predicted values for the cleaning success. In both figures, the points are close to a straight line, meaning that the model is well suited.

For the membranes from the flat-sheet batch, R^2 is 0.883 and for the membranes originated from the spiral-wound module, R^2 is 0.975. The value of R^2 is higher for the membranes originated from the spiral-wound module, indicating a better fit for the selected model. In both cases, R^2 is higher than 0.8, showing that the models have a high significance.

Q^2 gives an indication about the future prediction precision of the model. For the membranes originated from the spiral-wound module Q^2 is higher than 0.5, indicating that the model is rather good. For the membranes from the flat-sheet batch Q^2 is negative, denoting that the model does not have a predictive relevance.

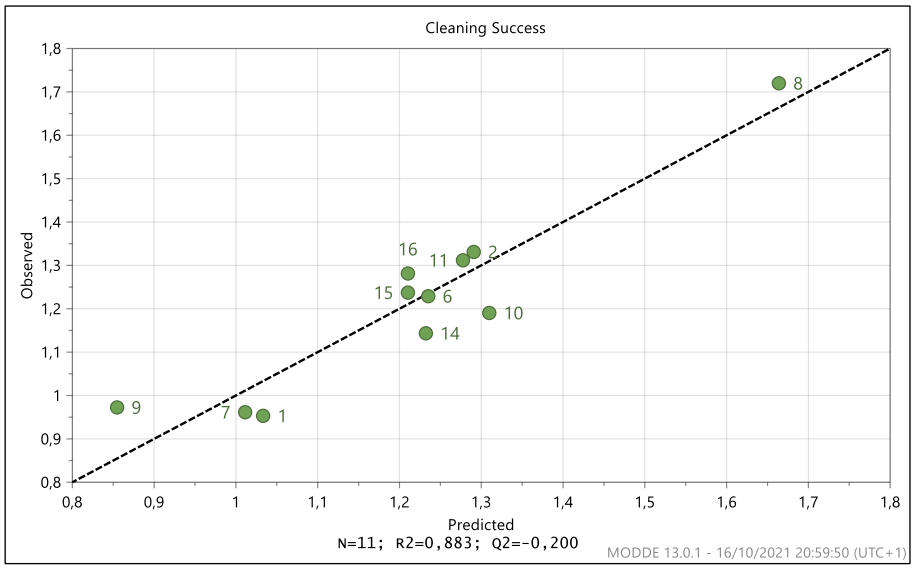

Figure 10 - Observed vs predicted plot of the membranes from the flat-sheet batch. N = actual runs, R2 = R squared, Q2 = Q squared.

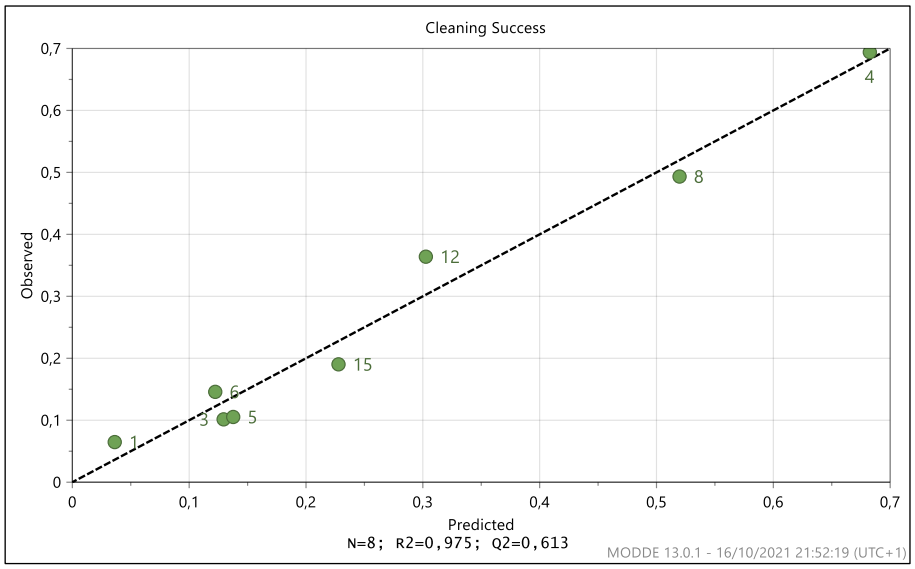

Figure 11 - Observed vs predicted plot of the membranes originated from the spiral-wound module. N = actual runs, R2 = R squared, Q2 = Q squared.

Figures 12 and 13 present the coefficient plots that evaluate the significance of the model terms. Even though it is more evident for the membranes from the flat-sheet batch, the cleaning agent concentration is the parameter that has the stronger impact on the cleaning success in both studies. The impact is positive and it means that an increase in concentration would likely result in an increase in cleaning success.

For the membranes from the flat sheet-batch, temperature and cleaning duration showed a low significance on the cleaning success, however, both impact the cleaning success positively (**Figure 12**). On the contrary, for the membranes originated from the spiral-wound module, the temperature seems to be almost as important as the cleaning agent concentration for a successful cleaning, while the

cleaning duration indicates a negative impact on the cleaning success (**Figure 13**). The negative impact of the cleaning duration is not reasonable but cannot be explained for now.

Coefficient plots (**Figures 12 and 13**) access the interaction between the factors as well. For the membranes from the flat sheet-batch, an interaction between concentration and temperature influences the cleaning success notably, while the interaction between concentration and duration is insignificant (**Figure 12**). For the membranes originated from the spiral-wound module, the interaction between concentration and temperature is as relevant as the interaction between concentration and duration, although the impact of the first is positive while the impact of the second is negative. This plot also reveals that the interaction between temperature and duration did not have any effect on the cleaning efficiency (**Figure 13**).

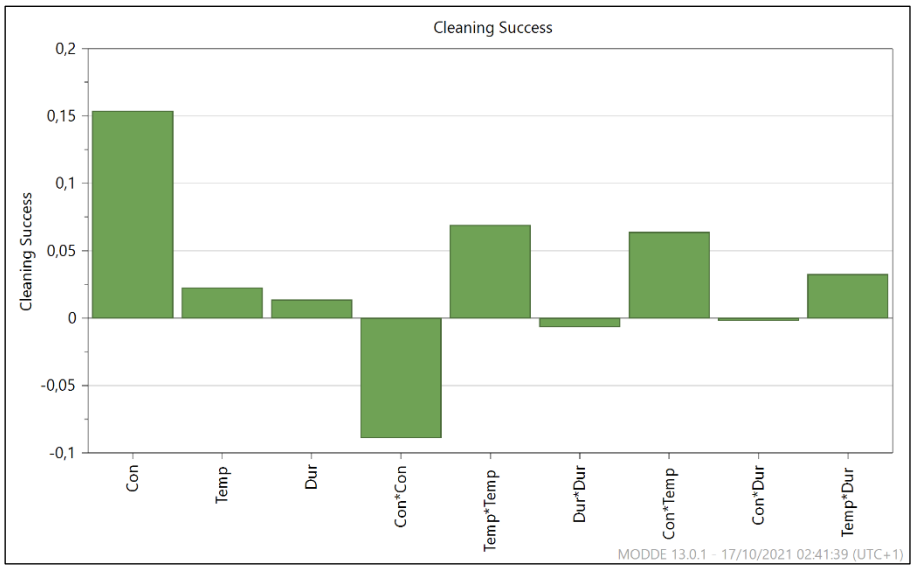

Figure 12 - Coefficient plot of the membranes from the flat sheet-batch.

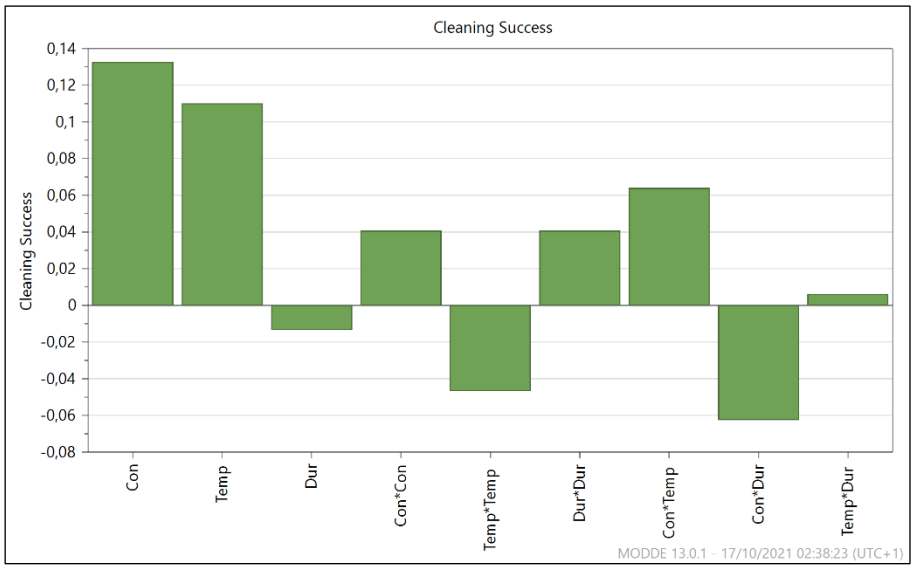

Figure 13 - Coefficient plot of the membranes originated from the spiral-wound module.

Figures 14 and 15 exhibit the cleaning success contour, illustrating the predicted response values. The dotted lines represent the selected values of the target, the minimum and the maximum cleaning success, 1, 0.3, and 1.3, respectively. For the membranes from the flat-sheet batch, a response within the desirable area (above the target and below the maximum) was achievable for a wide range of the three combined factors (**Figure 14**). However, the target was not reached for the membranes originated from the spiral-wound module, as shown in **Figure 15**.

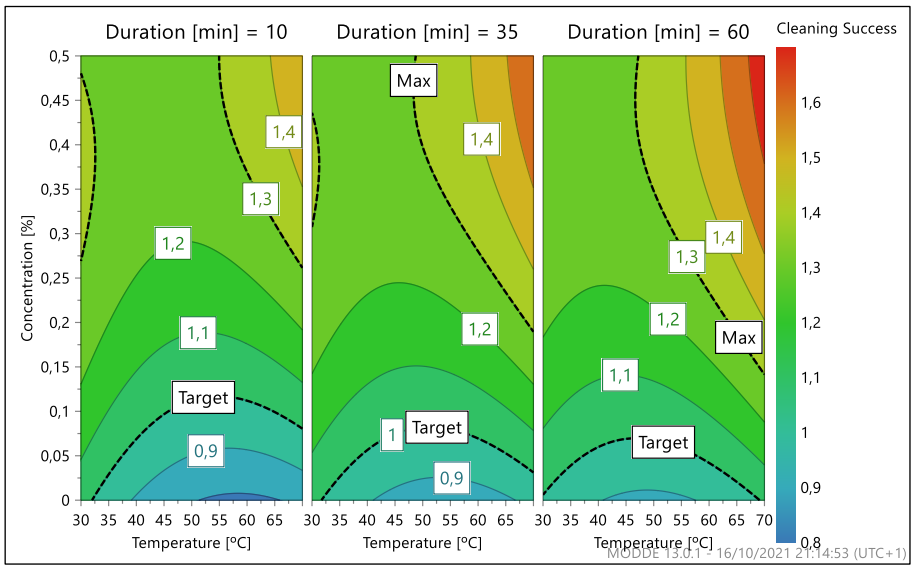

Figure 14 - Response contour plot of the membranes from the flat sheet-batch.

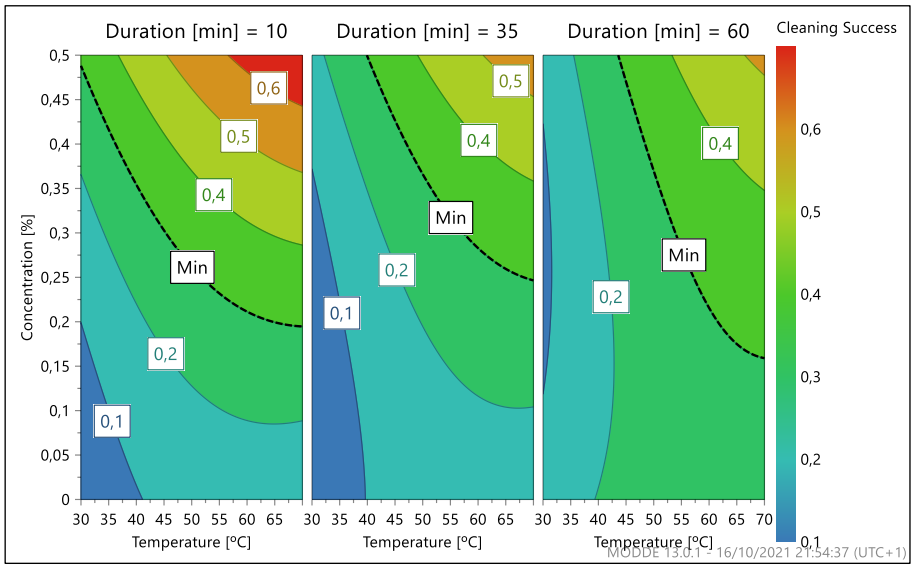

Figure 15 - Response contour plot of the membranes originated from the spiral-wound module.

Figures 16 and 17 express the design space that estimates the probability of success according to the response specifications and provides an area of operability. Inside the green area (area of operability), the probability of failure is less than 0.5%. For the membranes from the flat-sheet batch, a

response within that area is easily attainable even for the lowest values of the three combined cleaning parameters (**Figure 16**). Using values higher than the ones illustrated by the design space would only result in a waste of resources while cleaning. However, higher values of temperature and concentration are required when cleaning the membranes originated from the spiral-wound module, as seen in **Figure 17**. For those membranes, the green area is wider for a duration of 10 min (minimum duration), supporting the negative impact of this parameter on the cleaning success observed on **Figure 13**.

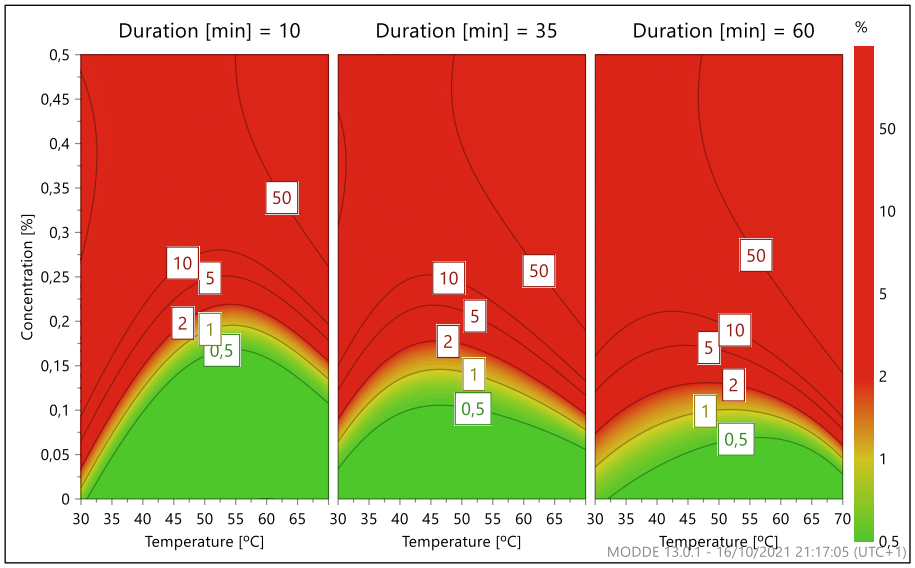

Figure 16 - Design space plot of the membranes from the flat sheet-batch.

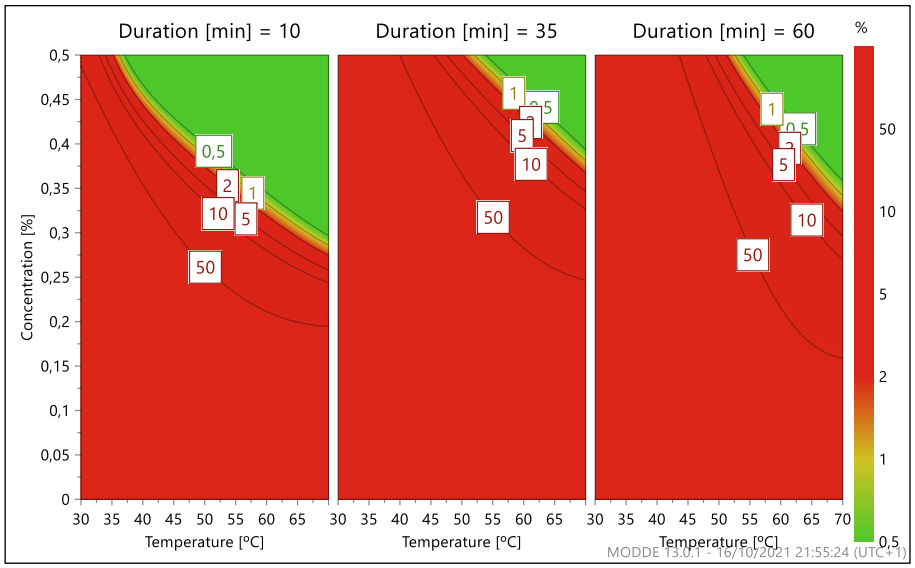

Figure 17 - Design space plot of the membranes originated from the spiral-wound module.

Overall, the analysis and predictions for the membranes from the flat-sheet batch are much more optimist than for the membranes originated from the spiral-wound module. Nevertheless, the selected model manifested a poor predictive relevance and a worse fit for the data from membranes

from the flat-sheet. On the other hand, the negative impact of the cleaning duration detected for the membranes originated from the spiral-wound module is not reasonable but cannot be explained for now. For the membrane from both batches, concentration of the cleaning agent appears to the be the most relevant cleaning parameter, whereas duration accused a rather low impact on cleaning success. The interaction between concentration and temperature revealed a remarkable influence in the cleaning success as well.

3.3. Membrane Analysis

The results from contact angle analysis, Fourier Transform Infrared Spectroscopy (FTIR) and Brunauer-Emmett-Teller (BET) analysis are expressed in the following subchapters.

3.3.1. Contact Angle Measurements

Contact angles of the membranes from all cleaning experiments were determined. For comparison reasons, also the contact angles of fouled and conditioned membranes were determined. A lower contact angle implies a higher hydrophilicity of the membrane, while a higher contact angle indicates a higher hydrophobicity of the membrane.

The results obtained on the membranes from the flat-sheet batch are displayed in **Table 9**. The contact angle of the fouled membrane (**Picture 18A**) is lower than the contact angle of the conditioned membrane (**Picture 18B**), meaning that the fouled membrane is more hydrophilic than the conditioned one. The main foulants present in thermomechanical pulping process water are polysaccharides **[15]** (hydrophilic) and extractives **[4]** (hydrophobic). For that reason, it is possible that the foulants remaining on membrane surface are mostly polysaccharides.

Table 9 - Contact angles of the membranes from the flat-sheet batch.

Experiment	Contact Angle
Conditioned	50.8˚
Fouled	46.1˚
1	56.2˚
2	50.4˚
3	50.5˚
4	55.1˚
5	43.7˚
6	50.8˚
7	44.3˚
8	47.6˚
9	50.2˚
10	55.0˚
11	53.6˚

Figure 18 - Contact angle comparison between a fouled membrane (**A**) and a conditioned membrane (**B**), both from the flat-sheet batch.

In experiment 5, 7, and 9, cleaning was conducted with pure water (0% of Ultrasil 10) and the contact angles of the membranes used in those experiments (**Figure 19A**) are lower than the ones measured on the membranes used in the other experiments (**Figure 19B**). The contact angles of the membranes used in experiment 5, 7, and 9 (**Figure 20A**) are also quite similar to one measured on the fouled membrane (**Figure 20B**). This suggests that cleaning with pure water barely changes the hydrophilicity of the fouled membranes, whereas cleaning with an Ultrasil 10 solution increases the hydrophobicity of the fouled membranes. A possible explanation is that by using Ultrasil 10, polysaccharides were removed in a larger scale than the extractives.

Figure 19 - Contact angle comparison between a membrane cleaned with pure water (**A**) and a membrane cleaned with an Ultrasil 10 solution (**B**), both from the flat-sheet batch.

Figure 20 - Contact angle comparison between a membrane cleaned with pure water (**A**) and a fouled membrane (**B**), both from the flat-sheet batch.

The results obtained on the membranes originated from the spiral-wound module are presented in **Table 10**. Once again, the contact angle measured on the fouled membrane (**Picture 21A**) is lower than the contact angle measured on the conditioned membrane (**Picture 21B**), meaning that the fouled membrane is more hydrophilic than the conditioned one. It suggests that the foulants remaining on membrane surface are mainly polysaccharides.

Table 10 - Contact angles of the membranes originated from the spiral-wound module.

Experiment	Contact Angle
Conditioned	60.1˚
Fouled	46.4˚
12	40.3˚
13	39.5˚
14	35.6˚
15	47.1˚
16	48.8˚
17	45.5˚
18	42.4˚
19	38.3˚

Figure 21 - Contact angle comparison between a fouled membrane (**A**) and a conditioned membrane (**B**), both from the spiral-wound module.

In experiment 12, 15, 16, 17 and 19, the cleaning was performed with an Ultrasil 10 solution and the contact angles of the membranes used in those experiments (**Figure 22A**) are similar to the one measured on the fouled membrane (**Figure 22B**). This indicates that cleaning with Ultrasil 10 barely changes the hydrophilicity of the fouled membranes, possibly due to an equal removal of both polysaccharides and extractives.

Figure 22 - Contact angle comparison between a fouled membrane (**A**) and a membrane cleaned with an Ultrasil 10 solution (**B**), both from the spiral-wound module.

Contact angle measurements indicate that the main foulants found on the membranes are probably polysaccharides, in the form of hemicelluloses, and that they are eliminated at some extent by cleaning with an Ultrasil 10 solution. Cleaning with pure water has not manifested any changes regarding

the hydrophilicity of the membrane, which can indicate that its cleaning efficiency was quite low. These observations also support the evaluation provided by DoE regarding the strong effect of the concentration of the cleaning agent on the cleaning performance.

3.3.2. Fourier Transform Infrared Spectroscopy

FTIR analysis were performed on the membranes from all cleaning experiments, and additionally on fouled and conditioned membranes, for comparison reasons.

The results obtained on the membranes from the flat-sheet batch are presented in **Figures 23 and 24**. **Figure 23** shows the FTIR spectra of a fouled, a conditioned and a cleaned membrane. Overall, the spectrum of the conditioned membrane is less accentuated than the other two spectra. The spectrum of the fouled membrane is quite similar to the spectrum of the cleaned membrane, although it is possible do detect some differences between the two.

There is a slight attenuation in peak intensity in the cleaned membrane compared to the fouled membrane at 1106, 1150, 1168, and 1653 cm^{-1}, and it can be interpretated as a signal of polysaccharides **[32-34]**. The attenuation in band intensity in the cleaned membrane compared to the fouled membrane from 3000 to 3400 cm^{-1} can be assign to polysaccharides as well **[35]**. The observation above suggests that the presence of polysaccharides on the fouled membrane surface were attenuated after cleaning. Finally, there are small variations in transmittance between the peaks at 1014 and 1080 cm^{-1}, which can result from both polysaccharides and PSU **[36,37]**, the polymer that the membranes used in this project are made of. Those peaks were attenuated in consequence of cleaning and for that reason, they are probably due to polysaccharides that were removed, since the amount of PSU on the membrane surface should not change after cleaning **[35]**.

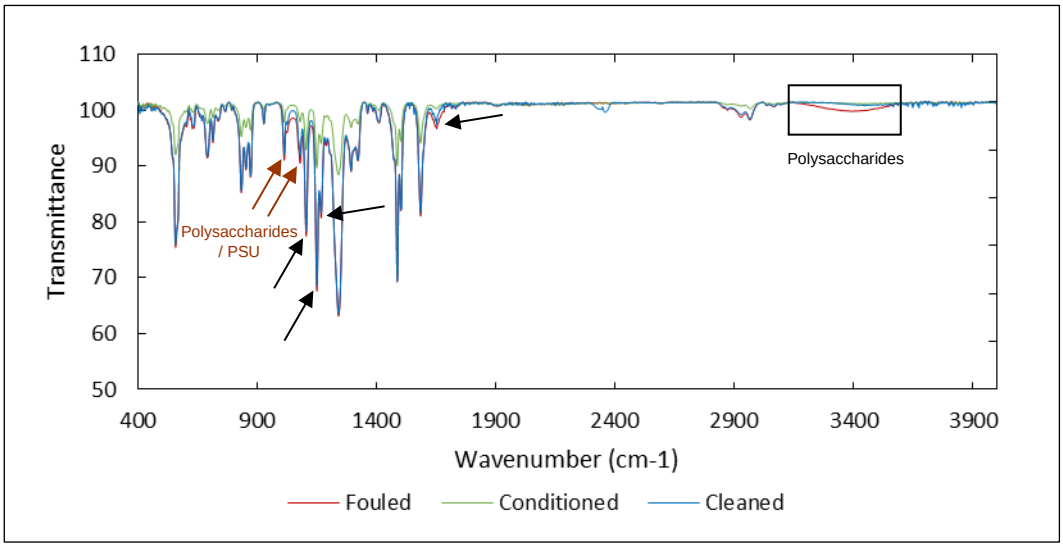

Figure 23 - FTIR spectra of a conditioned membrane, a fouled membrane, and a cleaned membrane, all from the flat-sheet batch.

Figure 24 shows FTIR spectra of three cleaned membranes: the ones that were exposed to the harshest cleaning (experiment 2), the mildest cleaning (experiment 7), and an average cleaning

(experiment 10). The difference between the spectra intensity is too small to allow an interpretation of the varying impact of the cleaning procedure on the fouling removal.

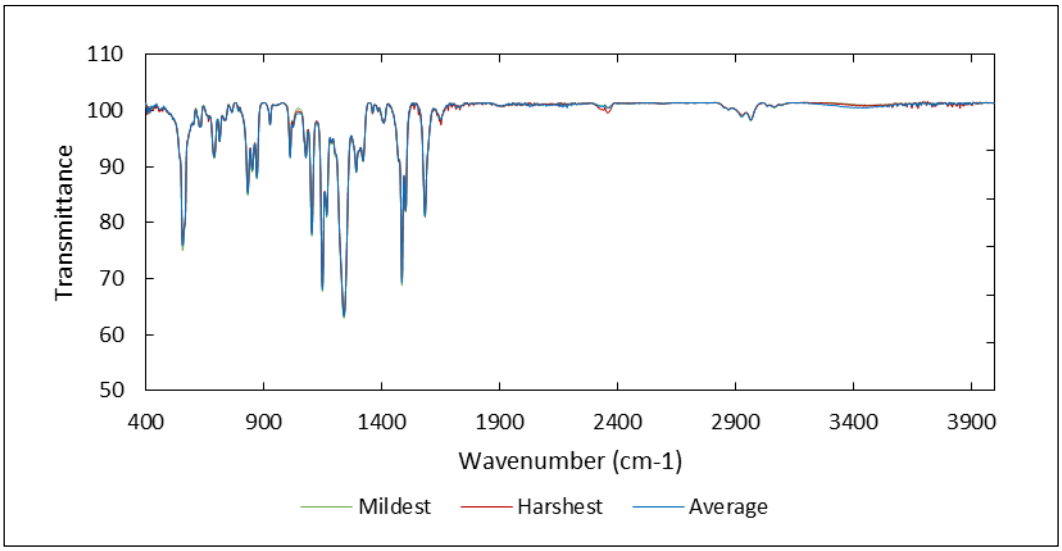

Figure 24 - FTIR spectra of three cleaned membranes after the harshest cleaning, the mildest cleaning, and an average cleaning, all from the flat-sheet batch.

The results obtained on the membranes originated from the spiral-wound module are showed in **Figures 25 and 26**. **Figure 25** shows FTIR spectra of a fouled, a conditioned and a cleaned membrane. Only small differences in transmittance are observed between the three spectra but interestingly, the peaks from the conditioned membrane are in general more intense than the other ones. This seems illogical because usually conditioned membranes display a spectrum with less peak intensity, since have not been exposed to the fouling solution, remaining pristine.

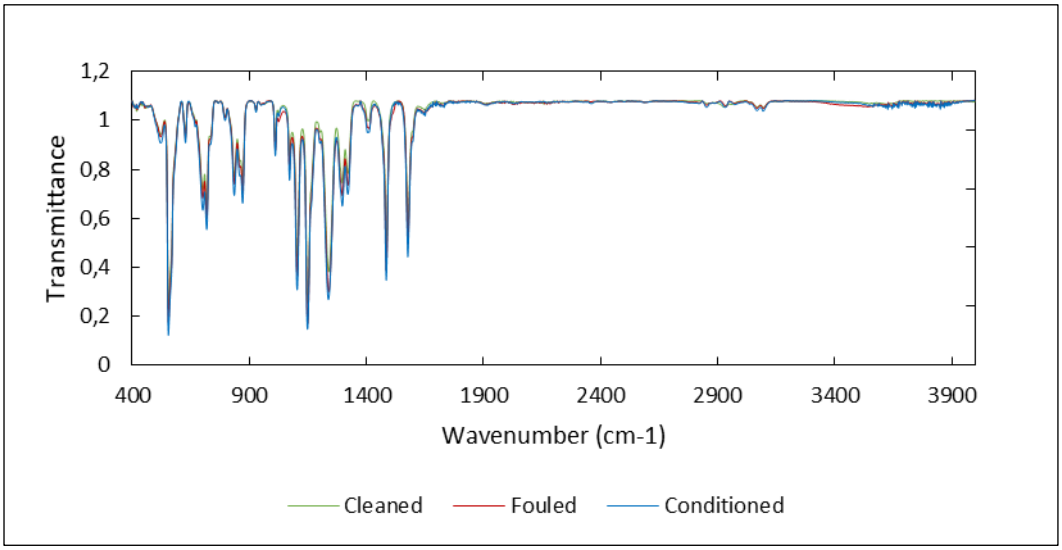

Figure 25 - FTIR spectra of a conditioned membrane, a fouled membrane, and a cleaned membrane, all from the spiral-wound module.

Figure 26 demonstrates FTIR spectra of three cleaned membranes: the ones that were exposed to the harshest cleaning (experiment 16), the mildest cleaning (experiment 18), and an average cleaning (experiment 17). Transmittance of the membrane after the harshest cleaning is almost identical to the transmittance of the membrane after the mildest cleaning. The membrane that was treated with an average cleaning presents a higher transmittance in the peaks, than the other two membranes.

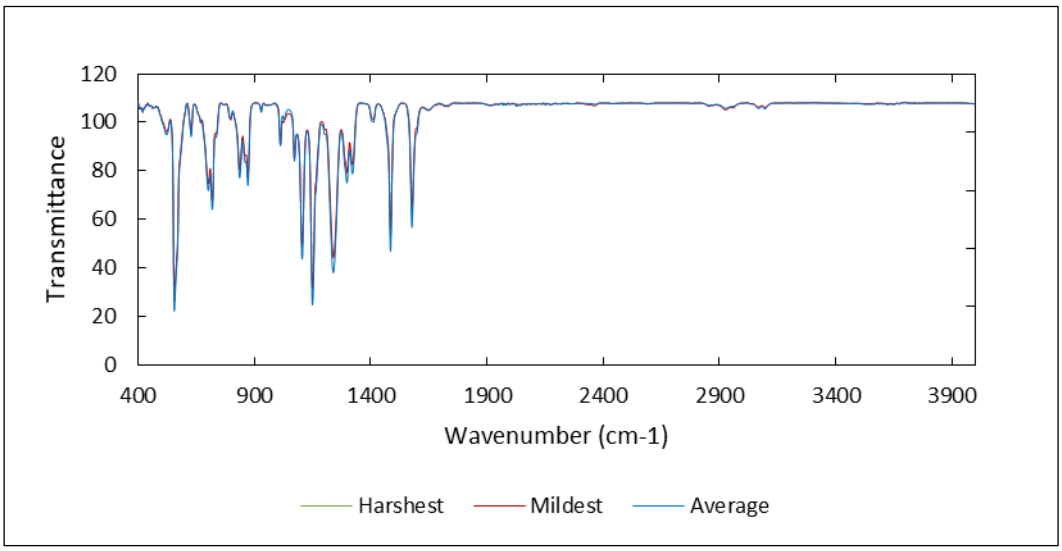

Figure 26 - FTIR spectra of three cleaned membranes after the harshest cleaning, the mildest cleaning, and the average cleaning, all from the spiral-wound module.

FTIR analysis reinforce the findings from the contact angle measurements, as polysaccharides appear to be the major foulants attached to the membrane surface and they seem to be partially removed by cleaning. It was not possible to achieve further interpretations regarding the differing influence of the cleaning procedure on the fouling removal based on this analytical method.

3.3.3. Brunauer-Emmett-Teller Analysis

BET analysis were conducted on a conditioned, a fouled, and three cleaned membranes for the membranes from both batches. The latter membranes were treated with the harshest cleaning, the mildest cleaning, and an average cleaning.

The pore area and pore volume as a function of pore diameter obtained on the membranes from the flat-sheet batch are presented in **Figures 27 and 28**. **Figure 27** shows the pore area distribution of the membrane samples and **Figure 28** displays the pore volume distribution of the membrane samples.

When comparing the distribution of the fouled membrane with the distribution of the conditioned membrane in both figures, a strong reduction in pore area can be observed and that comes along with a decrease in pore volume for all the pore widths. This could be due to considerable fouling caused by pore blocking **[38]**.

In both figures, it can be seen that the distributions of the three cleaned membranes are rather similar. For the smallest pores (< 9 nm) both, pore area and pore volume, are larger in the cleaned membranes, when compared to the conditioned and fouled membranes. Between 9 and 36 nm, pore area and pore volume distributions of the cleaned membranes are higher than the distribution of the

fouled membrane and lower than the distribution of the conditioned membrane. Finally, for a pore width bigger than 36 nm, pore area and pore volume are smaller for the cleaned membranes, when comparing with both conditioned and fouled membranes.

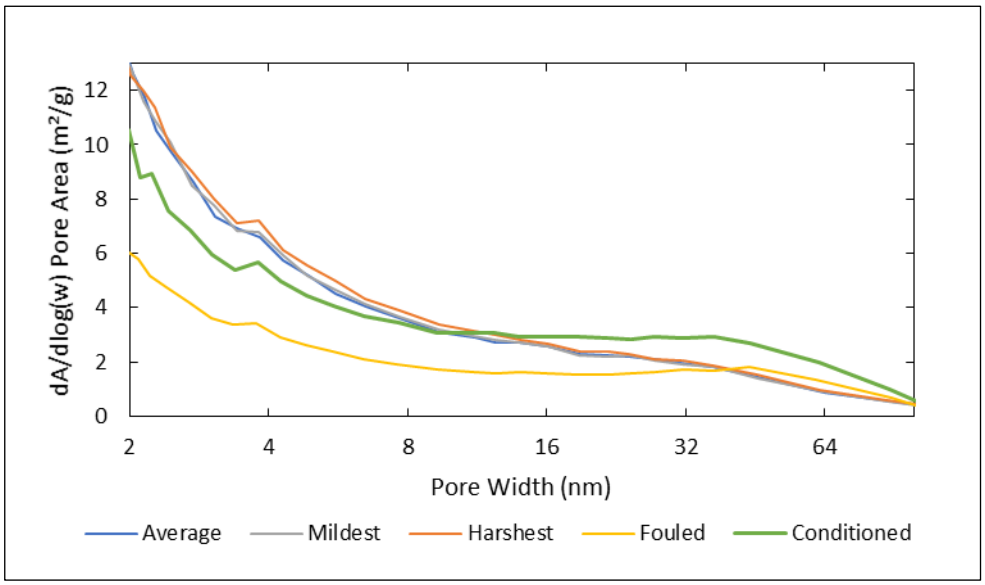

Figure 27 - BJH pore area as a function of pore diameter of a conditioned membrane, a fouled membrane and three cleaned membranes after the harshest cleaning, the mildest cleaning, and an average cleaning, all from the flat-sheet batch.

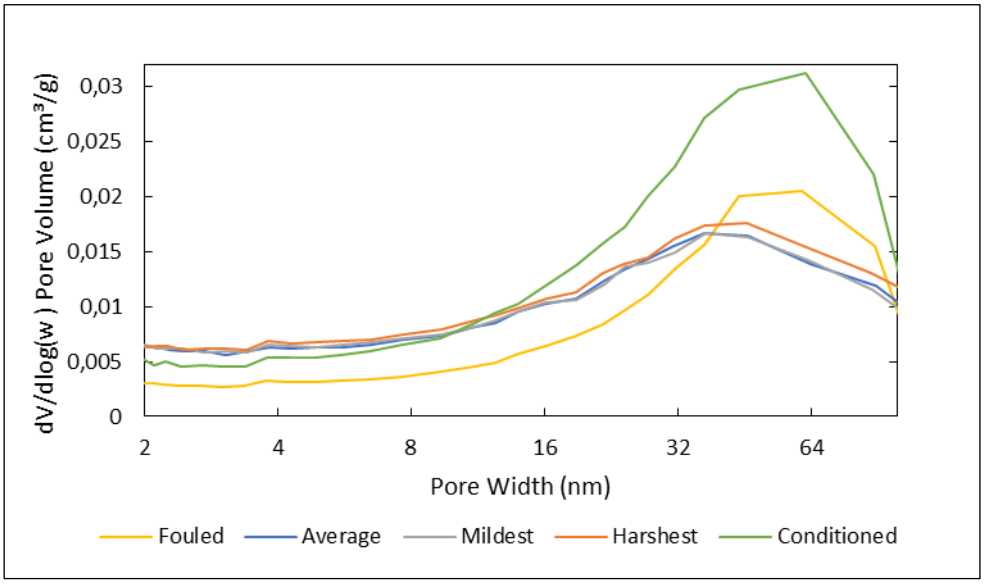

Figure 28 - BJH pore volume as a function of pore diameter of a conditioned membrane, a fouled membrane and three cleaned membranes after the harshest cleaning, the mildest cleaning, and an average cleaning, all from the flat-sheet batch.

The pore area and pore volume as a function of pore diameter of the membranes originated from the spiral-wound module are shown in **Figures 29 and 30**. **Figure 29** reveals the pore area distribution of the membrane samples and **Figure 30** shows the pore volume distribution of the membrane samples. When comparing the distribution of the fouled membrane with the distribution of

the conditioned membrane, a slight decrease in pore area for pores smaller than 22 nm can be seen, probably due to a little of fouling originated from pore blocking **[37]**. Regarding the pore volume, the distributions of the conditioned and the fouled membranes are very alike.

In both figures, it can be noticed that the distributions of the three cleaned membranes differ notably for pore widths smaller than 87 nm. For larger pore widths, the cleaning distributions become very similar for the three samples. For the pores between 12 and 65 nm both pore area and pore volume are bigger in the cleaned membranes, when compared to the conditioned and fouled membranes. For a pore width larger than 65 nm, pore area and pore volume are smaller for the cleaned membranes, when comparing with both conditioned and fouled membranes. These observations cannot be justified yet.

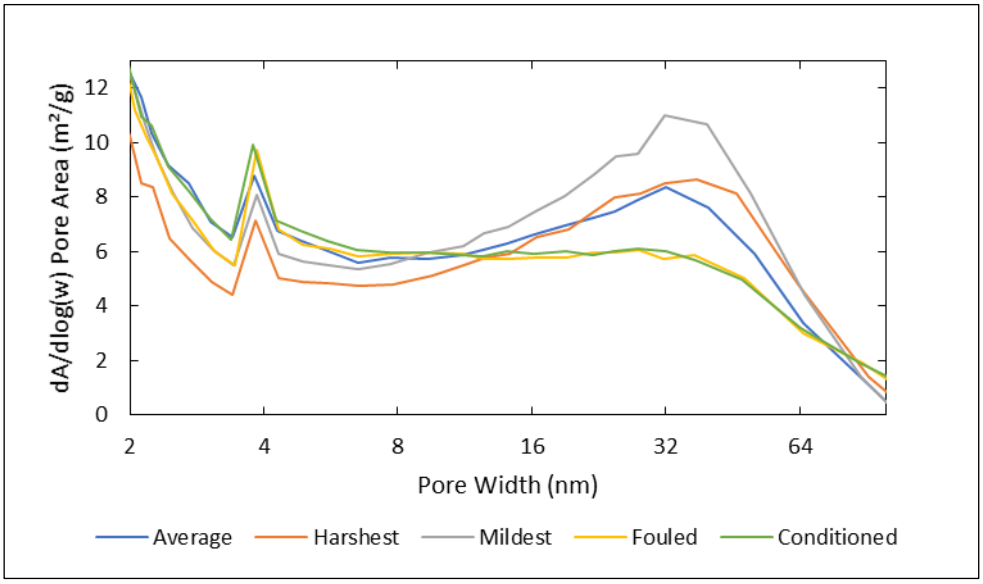

Figure 29 - BJH pore area as a function of pore diameter of a conditioned membrane, a fouled membrane and three cleaned membranes after the harshest cleaning, the mildest cleaning, and an average cleaning, all from the spiral-wound module.

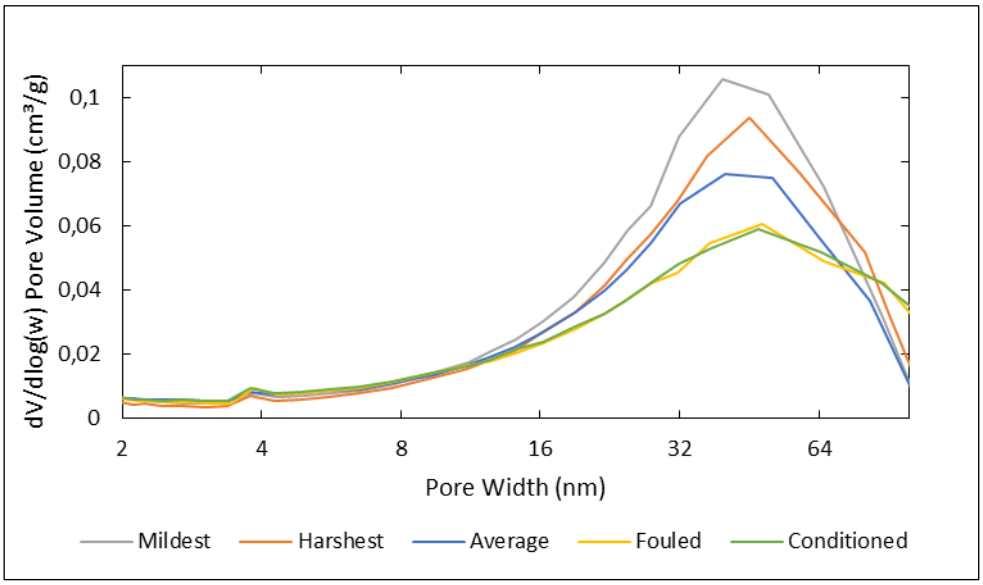

Figure 30 - BJH pore volume as a function of pore diameter of a conditioned membrane, a fouled membrane and three cleaned membranes after the harshest cleaning, the mildest cleaning, and an average cleaning, all from the spiral-wound module.

BET analysis only accused fouling in the form of pore blocking, possibly caused by polysaccharides molecules, based on the discoveries from the contact angle measurements and FTIR analysis. It was not possible to improve the knowledge about the varying effect of the cleaning procedure on the fouling removal based on this analytical method.

4. Conclusions

The objective of this thesis was to contribute to a deeper understanding about the impact of the parameters temperature, duration and concentration of a commonly used cleaning agent on the cleaning performance of membranes, providing an optimized cleaning protocol and a detailed examination on the structure and composition of a fouling layer caused by thermomechanical pulping process water.

This study was conducted on polysulfone membranes fouled with thermomechanical pulping process water by ultrafiltration. The impact of temperature, duration and concentration of the alkaline cleaning agent on the cleaning efficiency were investigate based on data flux analysis, using DoE.

Two DoE studies were developed, one for the membranes from a flat-sheet batch and another one for the membranes originated from a spiral-wound module. DoE evaluation was quite optimist regarding the analysis and predictions for the membranes from the flat-sheet batch when compared to the membranes originated from the spiral-wound module. According to DoE evaluation, a great cleaning success is achievable even for the lowest values of the three combined cleaning parameters, for the membranes from the flat-sheet batch. In both studies, the model showed a high significance, but it manifested a lack of predictive relevance for the data of membranes from the flat-sheet batch. On the other hand, the negative impact of the cleaning duration observed on study of the membranes originated from the spiral-wound module is not reasonable but cannot be explained for now. Besides, it is important to highlight that it is not accurate to assess the ability of a cleaning procedure based only on the maximized cleaning success. It is crucial to find a balance between a good cleaning success and a sustainable cost-effective cleaning protocol.

Overall, concentration of the cleaning agent proved to the be the most relevant cleaning parameter, while duration demonstrated a rather low impact on the cleaning success. The interaction between concentration and temperature appears to have a considerable effect on the cleaning success as well.

Lastly, the membrane surface and the fouling layer were analysed with contact angle measurements, FTIR and BET analysis.

Contact angle measurements suggest that the main foulants attached to the membrane surface are polysaccharides, in the form of hemicelluloses. They seem to be removed to some extent by cleaning with an alkaline cleaning solution. Contact angle measurements results also support the conclusions provided by DoE regarding the strong impact of the concentration of the cleaning agent on the cleaning efficiency, seeing that the membranes cleaned with pure water (0% of alkaline cleaning agent) have not manifested any changes concerning their hydrophilicity, indicating that this cleaning approach was inefficient.

FTIR analysis emphasizes the findings from the contact angle analysis, since polysaccharides seem to be the main foulants on the membrane surface. Based on the differences found in transmittance, they appear to be partly eliminated by cleaning.

BET analysis gave indications of fouling in the form of pore blocking. Based on the discoveries provided by the previous analyses this was likely caused by polysaccharides such as hemicelluloses.

The membrane analyses combined provided a comprehensive insight regarding the fouling layer composition and its impact on the membrane's inner area and volume. However, they have not contributed substantially for a better interpretation of the varying impact of the cleaning procedure on the fouling removal.

The findings of this work sustain the evidence that membrane fouling is an obstacle that can be overcome, encouraging a larger implementation of membrane technologies. This implementation would be a massive step towards a more sustainable and biobased society.

5. Future Perspectives

For future work, there are some different approaches that can be considered in conformity with this thesis.

Firstly, it would be interesting to extend this research with an optimization approach using DoE, based on the data obtained from the cleaning experiments conducted in this research. The goal is to establish an optimum cleaning protocol, that provides efficiency and cost-effectiveness.

It would be a great contribution to develop cleaning protocols based on long-term studies, to evaluate the effect on membrane aging and degradation. A harsh cleaning might be successful in terms of fouling removal, but it might also lead to negative impacts, including degradation of the membrane materials.

It would be important to carry out new studies similar to this one but focusing on the impact of other cleaning parameters on the membrane cleaning, such as CFV and TMP and for different cleaning agents as well. The combination of two different cleaning agents (e.g., alkaline and acid) could also be an appealing approach to consider in future investigations.

This work proved that for different types of membranes, different cleaning protocols should be conducted. For that reason, it would be useful to develop distinct researches for other membrane materials and geometries. Spiral-wound and hollow fibre modules are widely utilized in industry and it has been reported that they accuse a high fouling propensity and a low cleanability, due to their complex geometry. Having said that, cleaning experiments for those membrane modules should be carried out. Besides, it would be helpful to conduct a similar cleaning investigation on other polymeric membranes to evaluate if they would behave in a comparable way to PSU membranes.

Finally, it would be essential to perform cleaning studies under conditions that reproduce the industrial circumstances to ensure that the needs of industrial practices are fulfilled.

Actually, there is a constant need for new research concerning cleaning procedures as membrane technologies and cleaning agents evolve along with new environmental and economic challenges.

References

[1] Adnan, N.A.; Sapuan, S.; Ilyas, R.A. Pulp and paper production: A review. 2021

[2] Berg, J.E. (2008). Wood and Fibre Mechanics Related to the Thermomechanical Pulping Processes. PhD thesis, Mid Sweden University. 2008

[3] Persson, T.; Jönsson, A.S. Isolation of hemicelluloses by ultrafiltration of thermo-mechanical pulp process water - Influence of operating conditions. *Chemical Engineering Research & Design*, 88. 1548-1554, 2010

[4] Bokhary, A.; Cui, L.; Lin, H.J.; Liao, B.Q. A Review of Membrane Technologies for Integrated Forest Biorefinery. *Journal of Membrane Science & Research*, 3 120-141, 2017

[5] Thuvander, J.; Jönsson, A. S. Extraction of galactoglucomannan from thermomechanical pulp mill process water by microfiltration and ultrafiltration—Influence of microfiltration membrane pore size on ultrafiltration performance. *Chemical Engineering Research and Design*, 105. 10.1016, 2015

[6] Rudolph, G. Investigations on Membrane Fouling and Cleaning in Ultrafiltration Processes in Lignocellulosic Biorefineries. PhD thesis in Chemical Engineering, Lund University. 2021

[7] Jiang, L.; Li, P.; Wang, Y. Special Issue on “Novel Membrane Technologies for Traditional Industrial Processes”. *Processes*, 7. 144. 10.3390, 2019

[8] Hung, D.C.; Nguyen, N.C.; Uan, D.K.; Son, L.T. Membrane processes and their potential applications for freshwater provision in Vietnam. *Vietnam Journal of Chemistry,* 55(5): 533-544, 2017

[9] Bruggen, B.V.; Lejon, L.; Vandecasteele, C. Reuse, Treatment, and Discharge of the Concentrate of Pressure-Driven Membrane Processes. *Environmental Science and Technology*, 37(17):3733-8, 2003

[10] Mikhaylin, S.; Bazinet, L. Fouling on ion-exchange membranes: Classification, characterization and strategies of prevention and control. *Advances in Colloid and Interface Science*, 229. 10.1016, 2015

[11] Ramaswamy, S.; Huang, H.; Ramarao, B. *Separation and Purification Technologies in Biorefineries*. Wiley

[12] Virtanen, T.; Rudolph, G.; Lopatina, A. Analysis of membrane fouling by Brunauer-Emmet-Teller nitrogen adsorption/desorption technique. *Scientific Reports*, 10, 3427, 2020

[13] Wang, C.; Wei, A.; Wu, H.; Qu, F.; Chen, W.; Liang, H.; Li, G. Application of response surface methodology to the chemical cleaning process of ultrafiltration membrane. *Chinese Journal of Chemical Engineering*, 24, 651-657, 2016

[14] Regula, C.; Carretier, E.; Wyart, Y.; Gésan-Guiziou G.; Vincent, A.; Boudot, D.; Moulin, P.; Chemical cleaning/disinfection and ageing of organic UF membranes: a review. *Water Research*, 56:325-65, 2014

[15] Thuvander, J.; Zarebska, A.; Nielsen, C. H.; Jönsson, A.S. Characterization of Irreversible Fouling after Ultrafiltration of Thermomechanical Pulp Mill Process Water. *Journal of Wood Chemistry and Technology*, 38:3, 276-285, 2018

[16] Puro, L.; Kallioinen, M.; Mänttäri, M.; Nyström, M. Evaluation of behavior and fouling potential of wood extractives in ultrafiltration of pulp and paper mill process water. *Journal of Membrane Science*, 368. 150-158, 2011

[17] Luo, J.; Meyer, A.S.; Jonsson, G.; Pinelo, M. Enzyme immobilization by fouling in ultrafiltration membranes: Impact of membrane configuration and type on flux behaviour and biocatalytic conversion efficacy. *Biochemical Engineering Journal*, 83. 79-89, 2014

[18] Rana, D.; Matsuura, T.; Narbaitz, R.M.; Fenga, C. Development and characterization of novel hydrophilic surface modifying macromolecule for polymeric membranes. *Journal of Membrane Science*, 249. 103-112, 2005

[19] Chen, J.; Kim, S.L; Ting, Y.P.; Optimization of membrane physical and chemical cleaning by a statistically designed approach. *Journal of Membrane Science*, 219. 27-45, 2003

[20] Trägårdh, G. Membrane Cleaning. *Desalination*, 71(3), 325-335, 1989

[21] Kertész, Sz.; Freitas, T.; Hodúr, C. Characterization of polymer membranes by contact angle goniometer. *Analecta Technica Szegedinensia*, 8. 18-22, 2014

[22] Contact angle: Definition, meaning and measurement equipment. Retrieved from https:/ / www.linseis.com / en / properties / contact-angle /

[23] Ambroz, F.; Macdonald, T. J.; Martis, V.; Parkin, I. P. Evaluation of the BET Theory for the Characterization of Meso and Microporous MOFs. *Small Methods*, 2, 1800173, 2018

[24] Surface Area – Micromeritics. Retrieved from https:/ / www.micromeritics.com / particle-testing / analytical-testing / surface-area/

[25] What is DOE? Design of Experiments Basics for Beginners. Retrieved from https:// www.sartorius.com/en/knowledge/science-snippets/what-is-doe-design-of-experiments-basics-for-beginners-507170

[26] Sarabia, L.A.; Ortiz, M.C. Response Surface Methodology, *Comprehensive Chemometrics*, 2009

[27] Rudolph, G. QCM-D for studying Membrane Fouling – Opportunities and Limitations on the Example of Process Water from Thermomechanical Pulping in "Doctoral Dissertation, Investigation on Membrane Fouling and Cleaning in Ultrafiltration Processes in Lignocellulosic Biorefineries"

[28] Sluiter, A.; Hames, B.; Ruiz, R.; Scarlata, C.; Sluiter, J.; Templeton, D. Determination of Sugars, Byproducts, and Degradation of Products in Liquid Fraction Process Samples; Revised January 2008. 2006. Available online: https:/ / www.nrel.gov / docs / gen / fy08 / 42623.pdf

[29] Sluiter, A.; Hames, B.; Ruiz, R.; Scarlata, C.; Sluiter, J.; Templeton, D.; Crocker D. Determination of Structural Carbohydrates and Lignin in Biomass; Revised July 2011. 2008. Available online: https:/ / www.nrel.gov / docs / gen / fy13 / 42618.pdf

[30] Rudolph, G.; Hermansson, A.; Jönsson, A.S.; Lipnizki, F. In situ real-time investigations on adsorptive membrane fouling by thermomechanical pulping process water with quartz crystal microbalance with dissipation monitoring (QCM-D). *Separation and Purification Technology*, 254, 117578, 2021

[31] Humpert, D.; Ebrahimi, M.; Czermak, P. Membrane Technology for the Recovery of Lignin: A Review. *Membranes*, 6(3): 42, 2016

[32] Popescu, C.M.; Popescu, M.C.; Singurel, G.; Vasile, C.; Argyropoulos, D.; Willför, S. Spectral Characterization of Eucalyptus Wood. *Applied spectroscopy*, 61. 1168-77, 2007

[33] Kačuráková, M.; Capek, P.; Sasinkova, V.; Wellner, N.; Ebringerová, A. FT-IR study of plant cell wall model compounds: Pectic polysaccharides and hemicelluloses. *Carbohydrate Polymers*, 43. 195-203, 2007

[34] Karunakaran, C.; Rajkumar, R.; Bhargava K. Introduction to Biosensors. *Biosensors and Bioelectronics*, 1-68, 2015

[35] Rudolph, G.; Schagerlöf, H.; Krogh, K.B.M.; Jönsson, A.S.; Lipnizki, F. Investigations of Alkaline and Enzymatic Membrane Cleaning of Ultrafiltration Membranes Fouled by Thermomechanical Pulping Process Water. *Membranes*, 8(4), 91, 2018

[36] Wei, X.; Wang, Z.; Wang, J.; Wang, S. A novel method of surface modification to polysulfone ultrafiltration membrane by preadsorption of citric acid or sodium bisulfite. *Membrane Water Treatment*, 3. 35-49, 2012

[37] McCutcheon, J. R.; Hoek, E. M.V.; Bui, N.; Lind, M.L. Nanostructured Membranes for Engineered Osmosis Applications. WO/2011/060202, 2011

[38] Rudolph, G.; Virtanen, T.; Lopatina, A.; Schagerlöf, H.; Puro, L.; Kallioinen, M.; Lipnizki, F. Brunauer-Emmett-Teller analysis – a suitable method for membrane fouling in lignocellulosic biorefineries? Lund University

Annex

A. Ultrafiltration Solutions Analysis

Table A1 - Turbidity, dry solids and ash analysis of the feed solution (diluted retentate after MF of process water from thermomechanical pulping) and of the permeate and retentate after UF of the feed solution.

Solution	Sample	Turbidity	Dry Solids (mg/g)	Ash (mg/g)
Feed	1	410	4.58	0.00
	2	409	1.49	0.00
	3	409	1.49	0.00
	Average	409.3	2.52	0.00
	Standard Deviation	0.6	1.78	0.00
Retentate	1	320	12.27	0.00
	2	319	1.54	0.08
	3	320	1.56	0.06
	Average	319.7	5.12	0.05
	Standard Deviation	0.6	6.19	0.04
Permeate	1	1	0.09	0.06
	2	1	0.06	0.00
	3	1	0.14	0.07
	Average	1	0.10	0.04
	Standard Deviation	0	0.04	0.04

Table 11 - Lignin analysis of the feed solution (diluted retentate after MF of process water from thermomechanical pulping) and of the permeate and retentate after UF of the feed solution.

Solution	Sample	Klason Insoluble Lignin (mg/g)	Acid Soluble Lignin (g/L)	Total Lignin (g/L)
Feed	1	0.33	0.02	0.31
	2		0.02	0.31
	3		0.02	0.38
	Average	0.33	0.02	0.34
	Standard Deviation		0.00	0.03
Retentate	1	0.39	0.02	0.37
	2		0.02	0.36
	3		0.02	0.38
	Average	0.39	0.02	0.37
	Standard Deviation		0.00	0.01
Permeate	1	0.07	0.01	0.02
	2		0.01	0.02
	3		0.01	0.02
	Average	0.07	0.01	0.02
	Standard Deviation		0.00	0.00

Table 12 - Monosugars analysis of the feed solution (diluted retentate after MF of process water from thermomechanical pulping) and of the permeate and retentate after UF of the feed solution.

Solution	Sample	Arabinose (g/L)	Galactose (g/L)	Glucose (g/L)	Xylose (g/L)	Mannose (g/L)	Total Sugars (g/L)
Feed	1	0.03	0.16	0.17	−	0.30	0.65
	2	0.02	0.14	0.16	−	0.29	0.62
	3	0.02	0.13	0.14	−	0.28	0.58
	Average	0.02	0.14	0.16	0.00	0.29	0.62
	Standard Deviation	0.00	0.01	0.01		0.01	0.04
Retentate	1	0.17	0.61	0.66	0.00	1.30	2.74
	2	0.04	0.18	0.19	−	0.37	0.79
	3	0.04	0.18	0.20	−	0.39	0.81
	Average	0.08	0.32	0.35	0.00	0.69	1.44
	Standard Deviation	0.07	0.25	0.27		0.53	1.12
Permeate	1	0.37	−	0.06	−	−	0.43
	2	0.03	0.15	0.18	−	0.23	0.60
	3	0.03	0.14	0.16	−	0.25	0.59
	Average	0.15	0.15	0.13	0.00	0.24	0.54
	Standard Deviation	0.19	0.01	0.06		0.14	0.09

B. Linear Regression Lines of the Membranes from the Flat-sheet Batch

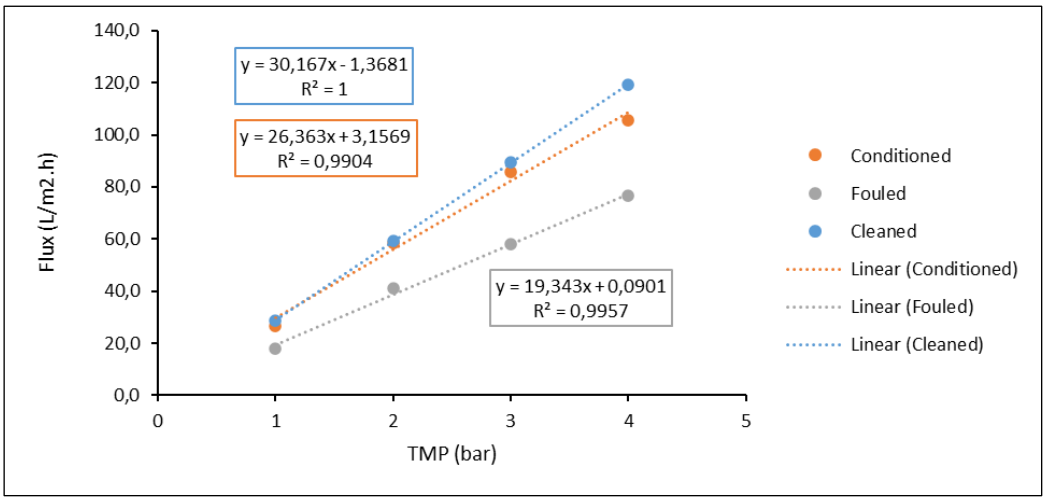

Figure 31 - Linear regression of the correlation between the average flux and the TMP of the conditioned membrane, the fouled membrane and the cleaned membrane - Experiment 1.

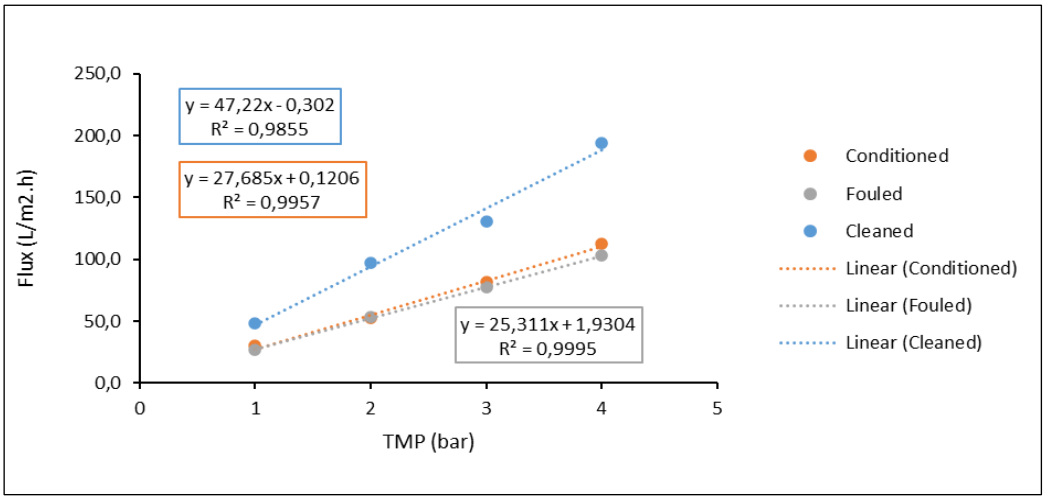

Figure 32 - Linear regression of the correlation between the average flux and the TMP of the conditioned membrane, the fouled membrane and the cleaned membrane - Experiment 2.

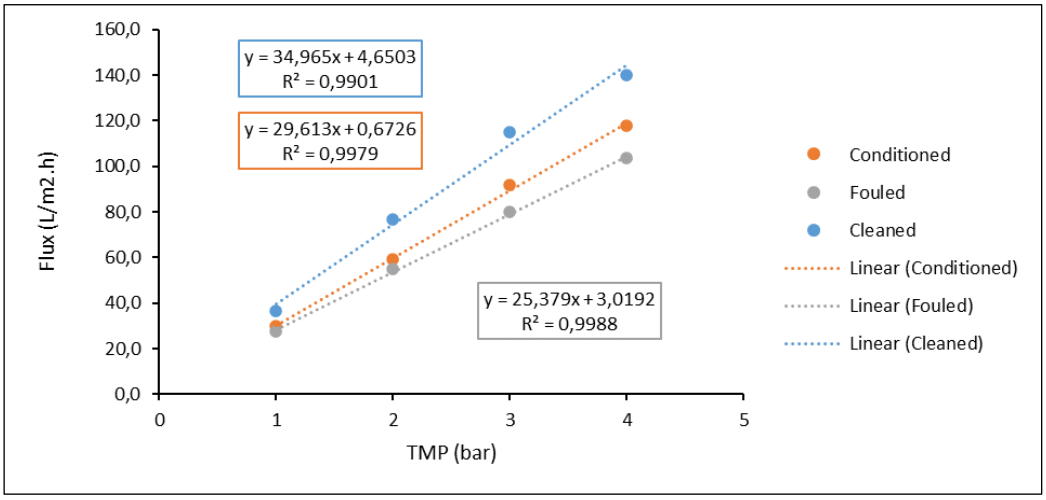

Figure 33 - Linear regression of the correlation between the average flux and the TMP of the conditioned membrane, the fouled membrane and the cleaned membrane - Experiment 3.

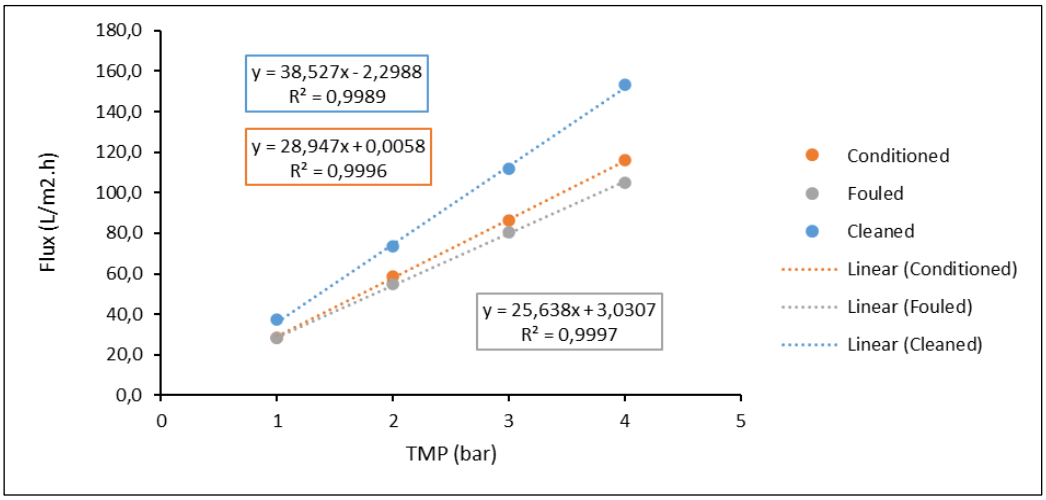

Figure 34 - Linear regression of the correlation between the average flux and the TMP of the conditioned membrane, the fouled membrane and the cleaned membrane - Experiment 4.

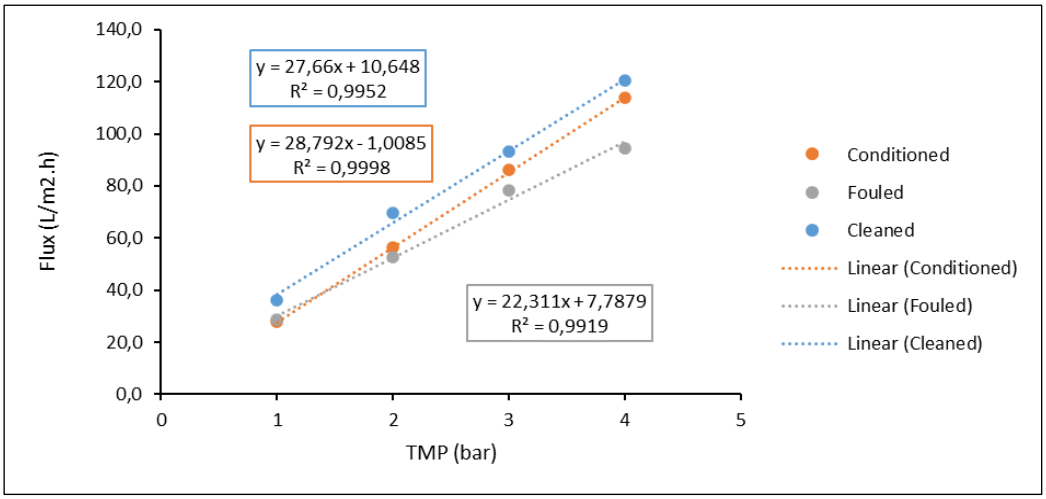

Figure 35 - Linear regression of the correlation between the average flux and the TMP of the conditioned membrane, the fouled membrane and the cleaned membrane - Experiment 5.

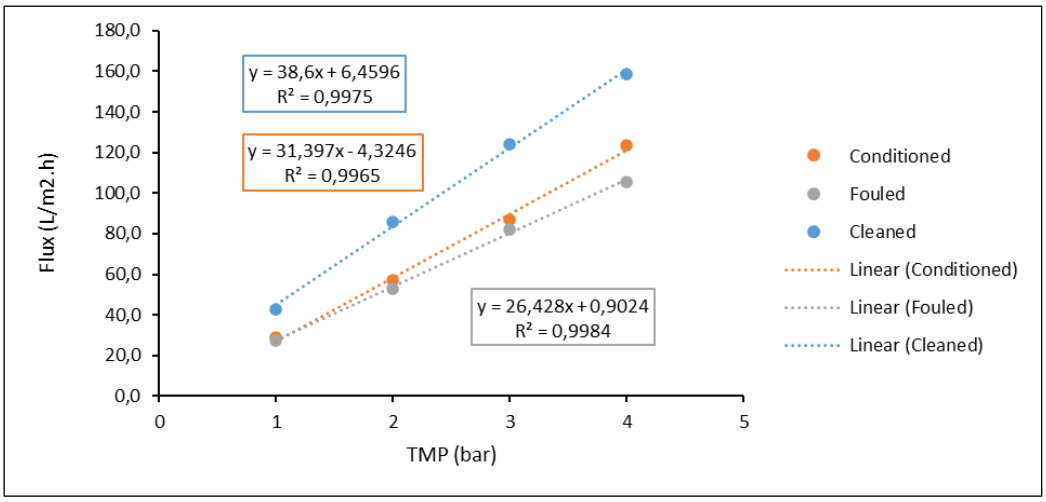

Figure 36 - Linear regression of the correlation between the average flux and the TMP of the conditioned membrane, the fouled membrane and the cleaned membrane - Experiment 6.

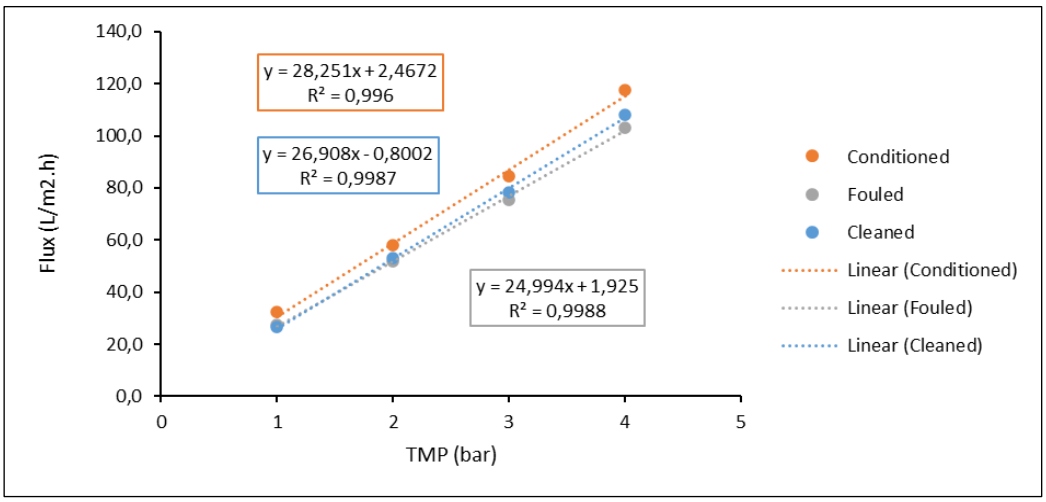

Figure 37 - Linear regression of the correlation between the average flux and the TMP of the conditioned membrane, the fouled membrane and the cleaned membrane - Experiment 7.

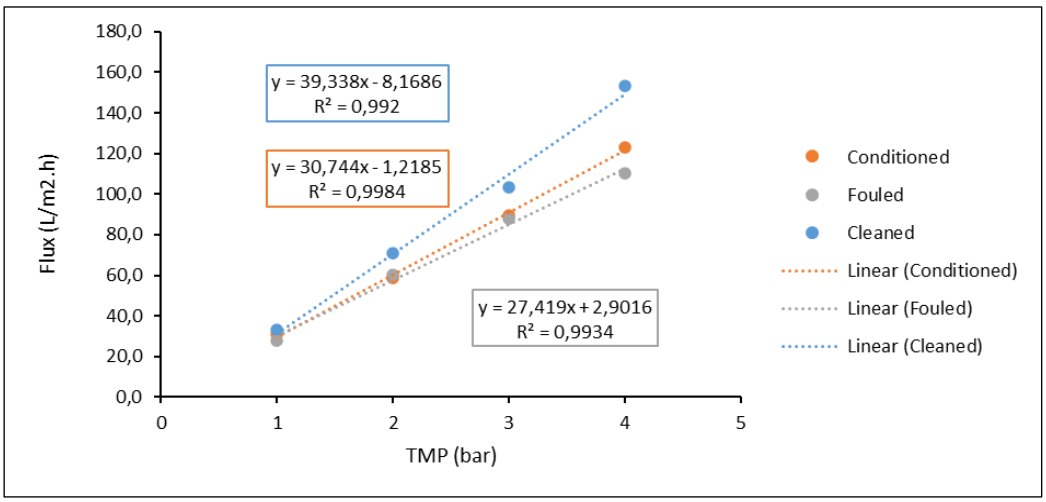

Figure 38 - Linear regression of the correlation between the average flux and the TMP of the conditioned membrane, the fouled membrane and the cleaned membrane - Experiment 8.

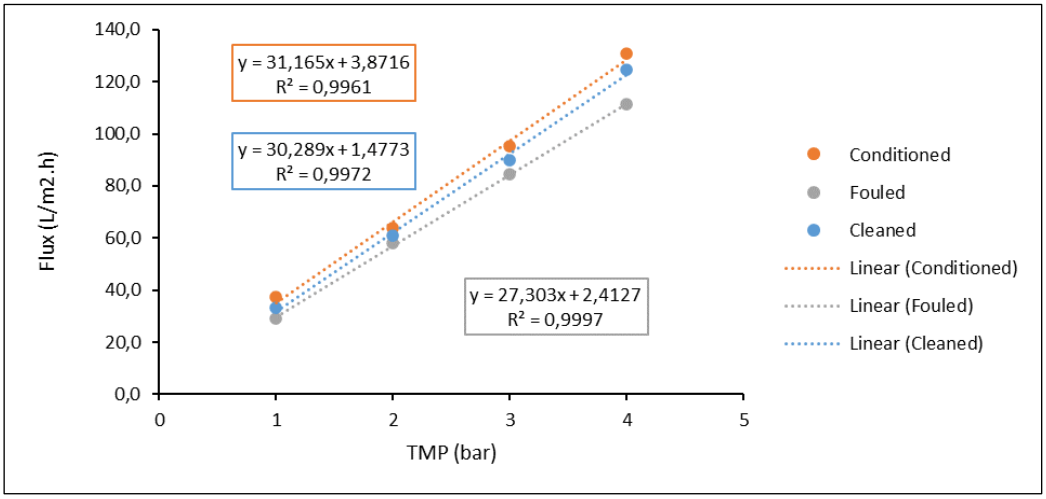

Figure 39 - Linear regression of the correlation between the average flux and the TMP of the conditioned membrane, the fouled membrane and the cleaned membrane - Experiment 9.

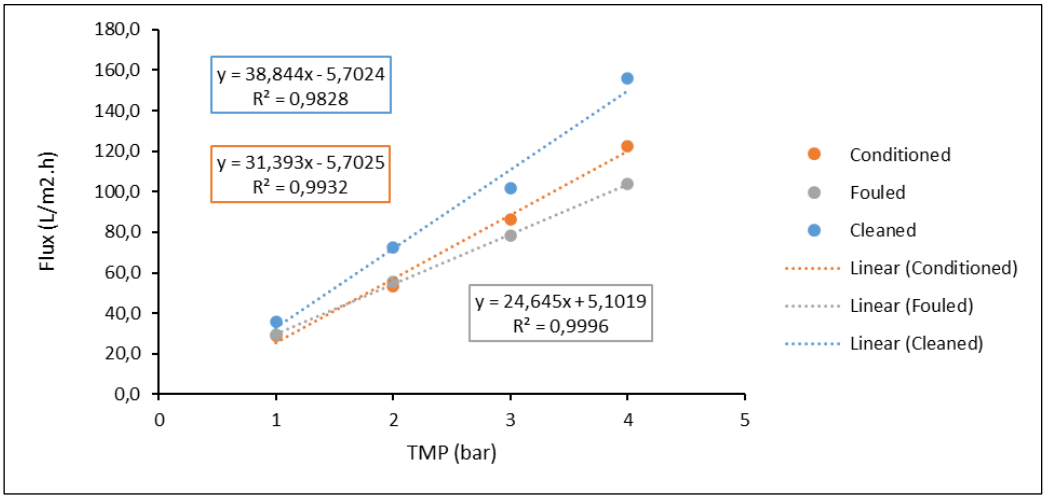

Figure 40 - Linear regression of the correlation between the average flux and the TMP of the conditioned membrane, the fouled membrane and the cleaned membrane - Experiment 10.

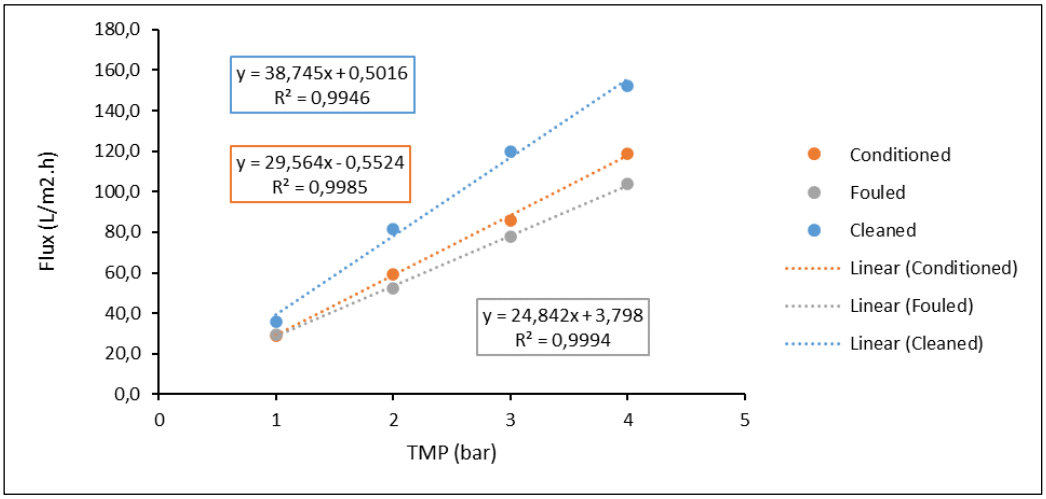

Figure 41 - Linear regression of the correlation between the average flux and the TMP of the conditioned membrane, the fouled membrane and the cleaned membrane - Experiment 11.

C. Linear Regression Lines of the Membranes Originated from the Spiral-wound Module

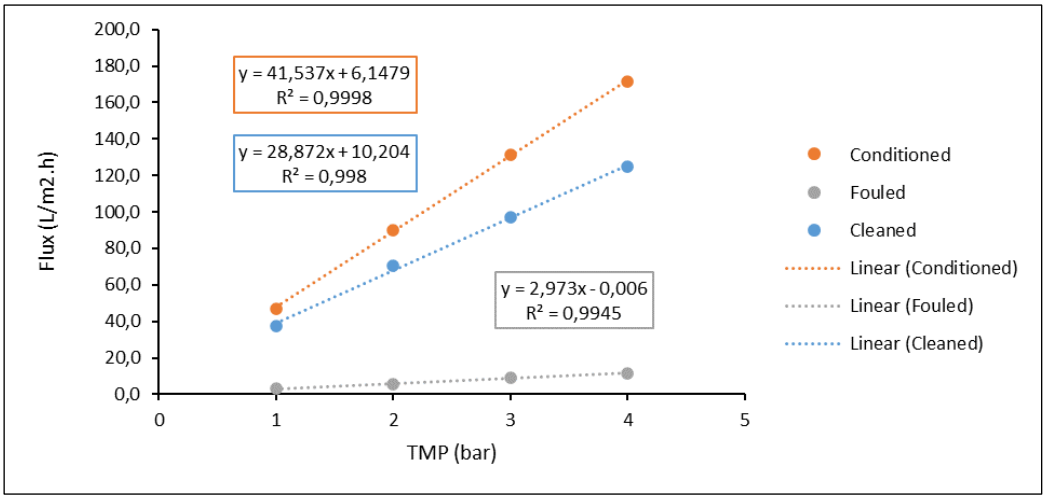

Figure C1 - Linear regression of the correlation between the average flux and the TMP of the conditioned membrane, the fouled membrane and the cleaned membrane - Experiment 12.

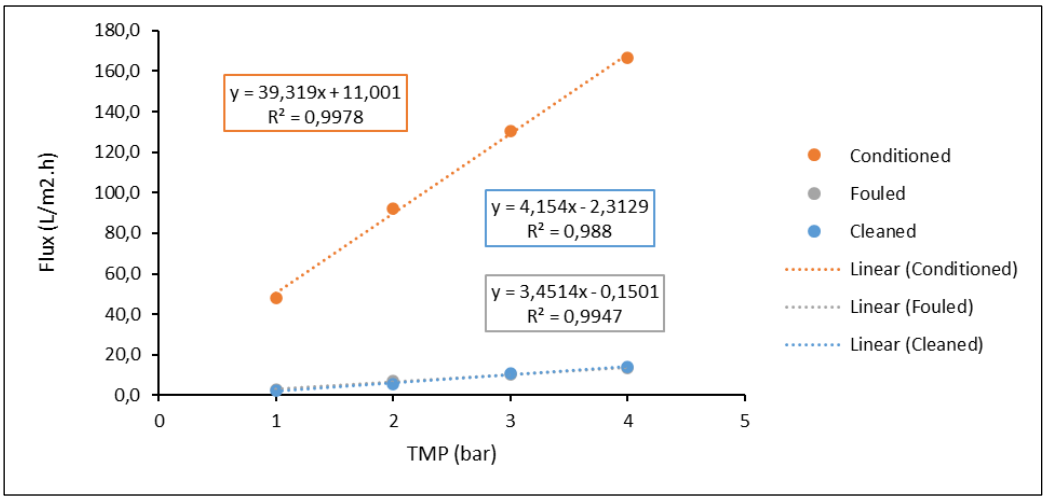

Figure C2 - Linear regression of the correlation between the average flux and the TMP of the conditioned membrane, the fouled membrane and the cleaned membrane - Experiment 13**.**

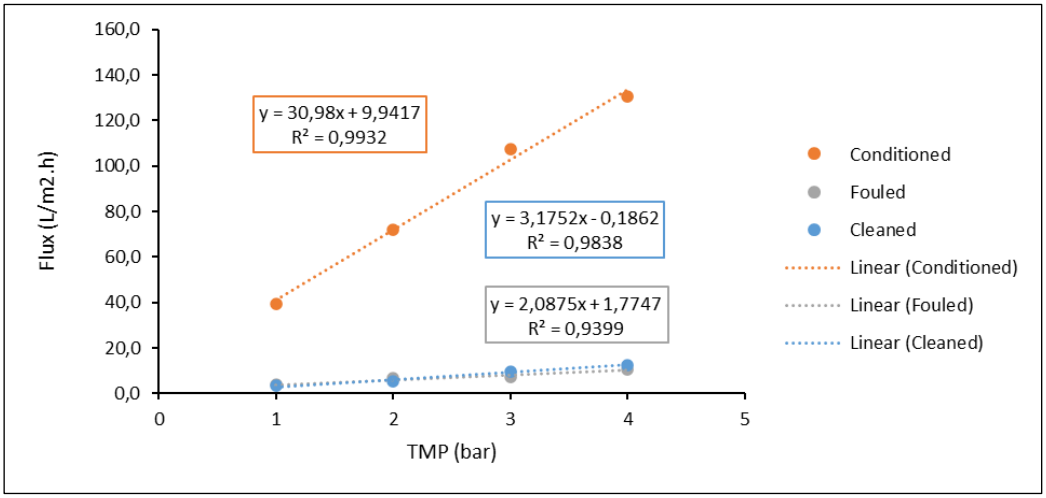

Figure C3 - Linear regression of the correlation between the average flux and the TMP of the conditioned membrane, the fouled membrane and the cleaned membrane - Experiment 14.

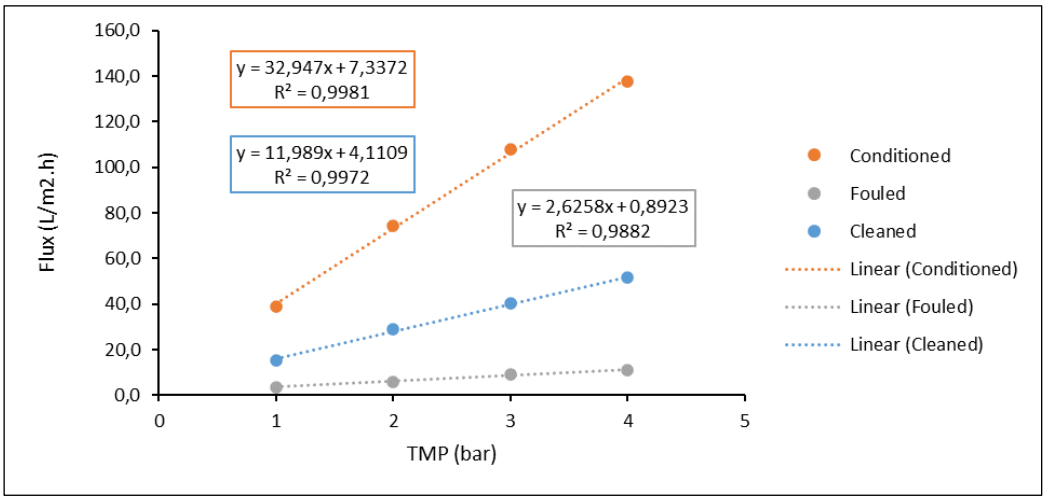

Figure C4 - Linear regression of the correlation between the average flux and the TMP of the conditioned membrane, the fouled membrane and the cleaned membrane - Experiment 15.

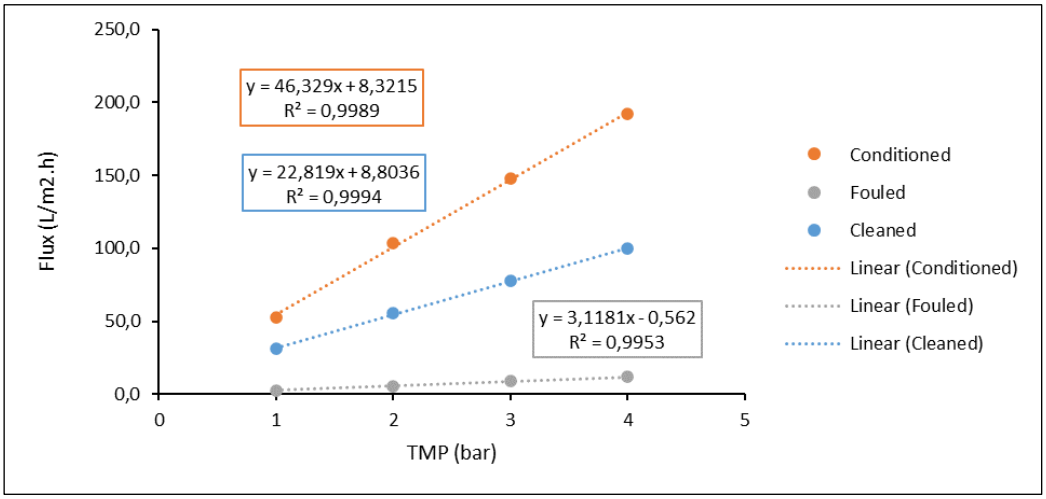

Figure C5 - Linear regression of the correlation between the average flux and the TMP of the conditioned membrane, the fouled membrane and the cleaned membrane - Experiment 16.

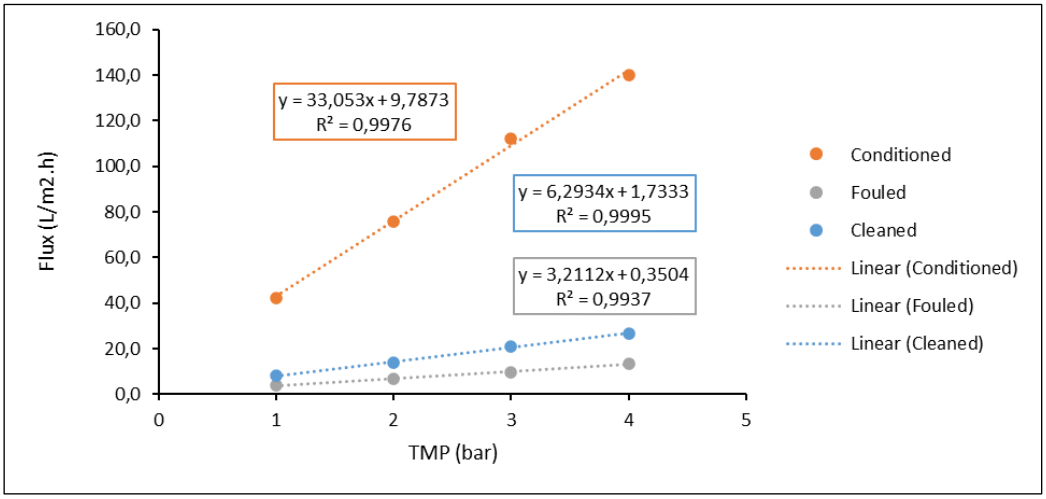

Figure C6 - Linear regression of the correlation between the average flux and the TMP of the conditioned membrane, the fouled membrane and the cleaned membrane - Experiment 17.

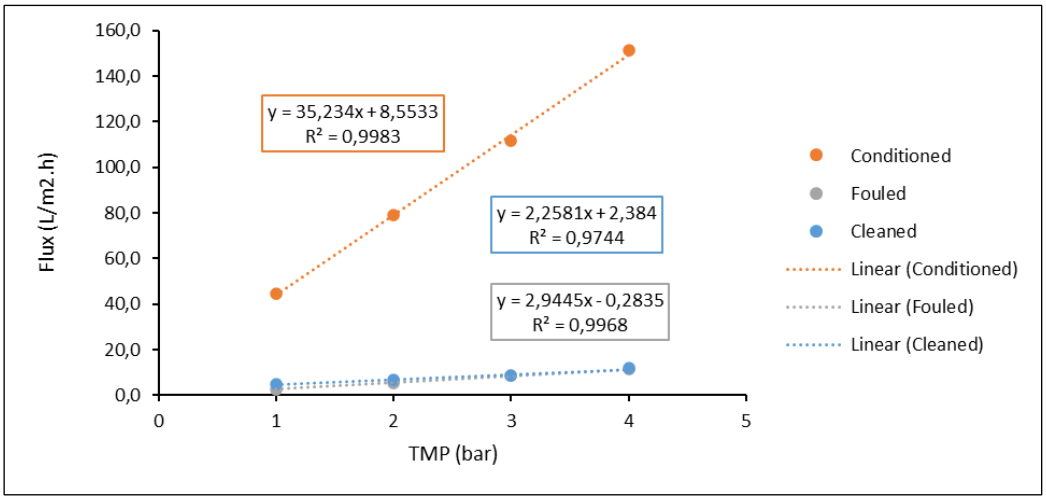

Figure C7 - Linear regression of the correlation between the average flux and the TMP of the conditioned membrane, the fouled membrane and the cleaned membrane - Experiment 18.

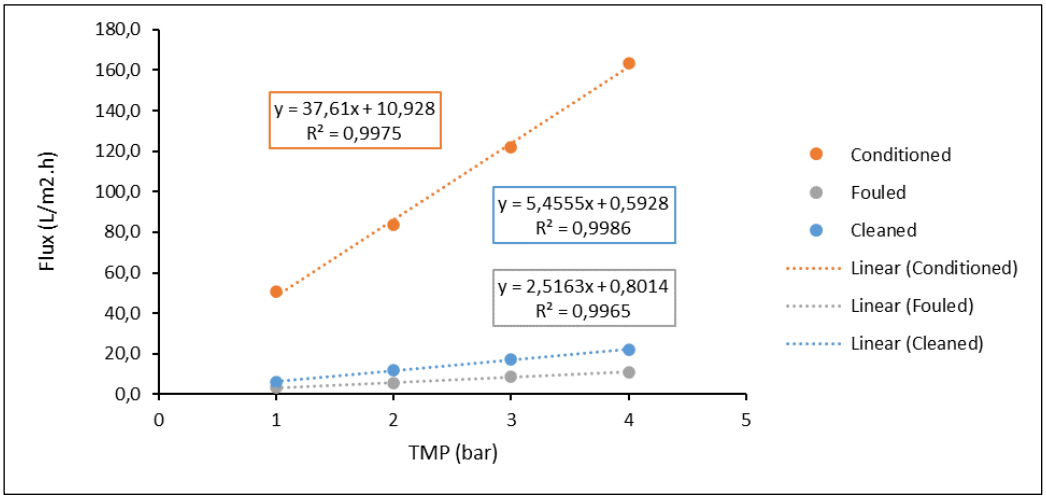

Figure C8 - Linear regression of the correlation between the average flux and the TMP of the conditioned membrane, the fouled membrane and the cleaned membrane - Experiment 19.